On the structure of Schnyder woods on orientable surfaces[*]

Daniel Gonçalves[†], Kolja Knauer[‡], Benjamin Lévêque[§]

July 5, 2016

Abstract

We propose a simple generalization of Schnyder woods from the plane to maps on orientable surfaces of higher genus. This is done in the language of angle labelings. Generalizing results of De Fraysseix and Ossona de Mendez, and Felsner, we establish a correspondence between these labelings and orientations and characterize the set of orientations of a map that correspond to such a Schnyder labeling. Furthermore, we study the set of these orientations of a given map and provide a natural partition into distributive lattices depending on the surface homology. This generalizes earlier results of Felsner and Ossona de Mendez. In the toroidal case, a new proof for the existence of Schnyder woods is derived from this approach.

1   Introduction

Schnyder [25] introduced Schnyder woods for planar triangulations with the following local property:

Definition 1.1 (Schnyder property) *Given a map G, a vertex v and an orientation and coloring[1] of the edges incident to v with the colors 0, 1, 2, we say that v satisfies the* Schnyder property, *(see Figure 1) if v satisfies the following local property:*

- *Vertex v has out-degree one in each color.*

- *The edges $e_0(v)$, $e_1(v)$, $e_2(v)$ leaving v in colors 0, 1, 2, respectively, occur in counterclockwise order.*

[1]Throughout the paper colors and some of the indices are given modulo 3.

- *Each edge entering v in color i enters v in the counterclockwise sector from $e_{i+1}(v)$ to $e_{i-1}(v)$.*
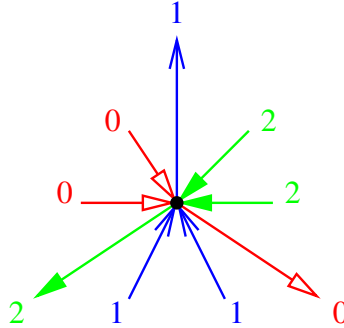

Figure 1: The Schnyder property. The depicted correspondence between red, blue, green, 0, 1, 2, and the arrow shapes will be used through the paper.

Definition 1.2 (Schnyder wood) *Given a planar triangulation G, a* Schnyder wood *is an orientation and coloring of the inner edges of G with the colors 0, 1, 2 (edges are oriented in one direction only), where each inner vertex v satisfies the* Schnyder *property.*

See Figure 2 for an example of a Schnyder wood.
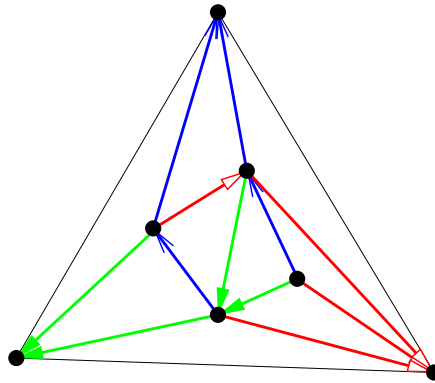
Figure 2: Example of a Schnyder wood of a planar triangulation.

Schnyder woods are today one of the main tools in the area of planar graph representations. Among their most prominent applications are the following: They provide a machinery to construct space-efficient straight-line drawings [26, 18, 8], yield a characterization of planar graphs via the dimension of their vertex-edge incidence poset [25, 8], and are used to encode triangulations [23, 3]. Further applications lie in enumeration [4], representation by geometric objects [13, 16], graph spanners [5], etc. The richness of

these applications has stimulated research towards generalizing Schnyder woods to non planar graphs.

For higher genus triangulated surfaces, a generalization of Schnyder woods has been proposed by Castelli Aleardi, Fusy and Lewiner [6], with applications to encoding. In this definition, the simplicity and the symmetry of the original definition of Schnyder woods are lost. Here we propose an alternative generalization of Schnyder woods for higher genus that generalizes the one proposed in [17] for the toroidal case.

A closed curve on a surface is *contractible* if it can be continuously transformed into a single point. Except if stated otherwise, we consider graphs embedded on orientable surfaces such that they do not have contractible cycles of size 1 or 2 (i.e. no contractible loops and no contractible double edges). Note that this is a weaker assumption, than the graph being *simple*, i.e. not having *any* cycles of size 1 or 2 (i.e. no loops and no multiple edges). A graph embedded on a surface is called a *map* on this surface if all its faces are homeomorphic to open disks. A map is a triangulation if all its faces are triangles.

In this paper we consider finite maps. We denote by n be the number of vertices and m the number of edges of a graph. Given a graph embedded on a surface, we use f for the number of faces. Euler's formula says that any map on an orientable surface of genus g satisfies $n - m + f = 2 - 2g$. In particular, the plane is the surface of genus 0, the torus the surface of genus 1, the double torus the surface of genus 2, etc. By Euler's formula, a triangulation of genus g has exactly $3n + 6(g - 1)$ edges. So having a generalization of Schnyder woods in mind, for all $g \geq 2$ there are too many edges to force all vertices to have outdegree exactly three. This problem can be overcome by allowing vertices to fulfill the Schnyder property "several times", i.e. such vertices have outdegree 6, 9, etc. with the color property of Figure 1 repeated several times (see Figure 3).

Outdegree six   Outdegree nine

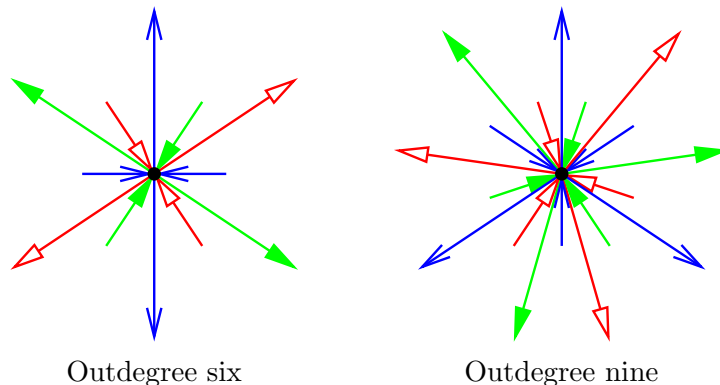Figure 3: The Schnyder property repeated several times around a vertex.

Figure 4 is an example of such a Schnyder wood on a triangulation of the double torus. The double torus is represented by a fundamental polygon – an octagon. The sides of the octagon are identified according to their labels. All the vertices of the triangulation have outdegree three except two vertices, the circled ones, that have outdegree six. Each

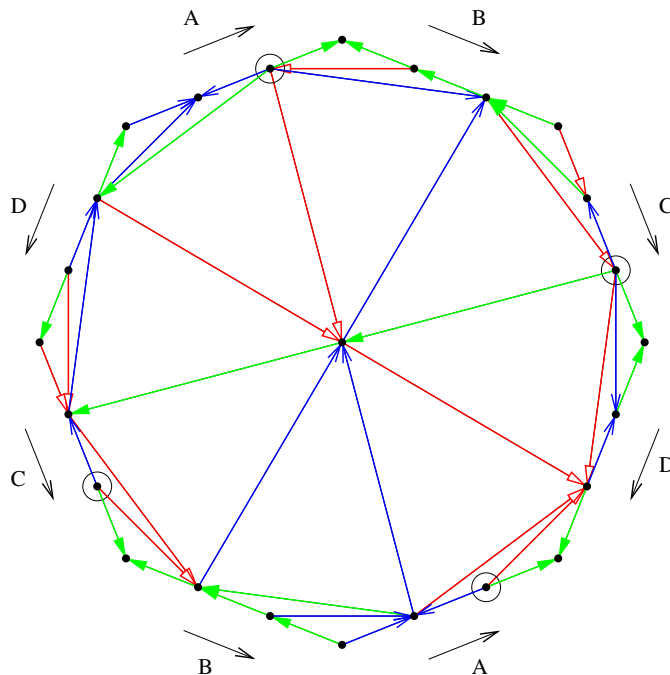of the latter appear twice in the representation.

Figure 4: A Schnyder wood of a triangulation of the double torus.

In this paper we formalize this idea to obtain a concept of Schnyder woods applicable to general maps (not only triangulations) on arbitrary orientable surfaces. This is based on the definition of Schnyder woods via angle labelings in Section 2. We prove several basic properties of these objects. While every map admits a "trivial" Schnyder wood, the existence of a non-trivial one remains open but leads to interesting conjectures.

By a result of De Fraysseix and Ossona de Mendez [14], for any planar triangulation there is a bijection between its Schnyder woods and the orientations of its inner edges where every inner vertex has outdegree three. Thus, any orientation with the proper outdegree corresponds to a Schnyder wood and there is a unique way, up to symmetry of the colors, to assign colors to the oriented edges in order to fulfill the Schnyder property at every inner vertex. This is not true in higher genus as already in the torus, there exist orientations that do not correspond to any Schnyder wood (see Figure 5). In Section 3, we characterize orientations that correspond to our generalization of Schnyder woods.

In Section 4, we study the transformations between Schnyder orientations. We obtain a partition of the set of Schnyder woods into homology classes of orientations, each of these classes being a distributive lattice. This generalizes corresponding results obtained for the plane by Ossona de Mendez [22] and Felsner [10]. The particular properties of the minimal element of such a lattice recently led to an optimal linear encoding method for toroidal triangulations by Despré, the first author, and the third author [7]. This generalizes previous results of Poulalhon and Schaeffer for the plane [23].
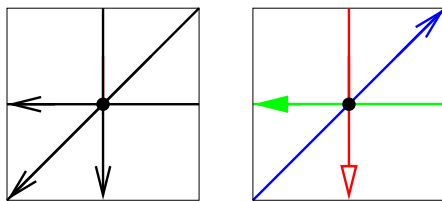
Figure 5: Two different orientations of a toroidal triangulation. Only the one on the right corresponds to a Schnyder wood.

In Section 5, we focus on toroidal triangulations. We use the characterization theorem of Section 3 to give a new proof of the existence of Schnyder woods in this case. We show that the so-called "crossing" property allows to define a canonical lattice. Note that this special lattice is the one used in [7] to obtain a bijection. Finally the results of the paper are illustrated by an example.

2 Generalization of Schnyder woods

2.1 Angle labelings

Consider a map G on an orientable surface. An *angle labeling* of G is a labeling of the angles of G (i.e. face corners of G) in colors 0, 1, 2. More formally, we denote an angle labeling by a function $\ell : \mathcal{A} \to \mathbb{Z}_3$, where $\mathcal{A}$ is the set of angles of G. Given an angle labeling, we define several properties of vertices, faces and edges that generalize the notion of Schnyder angle labeling in the planar case [12].

Consider an angle labeling ℓ of G. A vertex or a face v is of *type k*, for $k \geq 1$, if the labels of the angles around v form, in counterclockwise order, $3k$ nonempty intervals such that in the j-th interval all the angles have color $(j \mod 3)$. A vertex or a face v is of *type 0*, if the labels of the angles around v are all of color i for some i in $\{0, 1, 2\}$.

An edge e is of *type 1 or 2* if the labels of the four angles incident to edge e are, in clockwise order, $i-1, i, i, i+1$ for some i in $\{0, 1, 2\}$. The edge e is of *type 1* if the two angles with the same color are incident to the same extremity of e and of *type 2* if the two angles are incident to the same side of e. An edge e is of *type 0* if the labels of the four angles incident to edge e are all i for some i in $\{0, 1, 2\}$ (See Figure 6).

If there exists a function $f : V \to \mathbb{N}$ such that every vertex v of G is of type $f(v)$, we say that ℓ is f-VERTEX. If we do not want to specify the function f, we simply say that ℓ is VERTEX. We sometimes use the notation K-VERTEX if the labeling is f-VERTEX for a function f with $f(V) \subseteq K$. When $K = \{k\}$, i.e. f is a constant function, then we use the notation k-VERTEX instead of f-VERTEX. Similarly we define FACE, K-FACE, k-FACE, EDGE, K-EDGE, k-EDGE.

The following lemma expresses that property EDGE is the central notion here. Properties K-VERTEX and K-FACE are used later on to express additional requirements on

the angle labelings that are considered.

Lemma 2.1 *An* EDGE *angle labeling is* VERTEX *and* FACE.

Proof. Let ℓ be an EDGE angle labeling. Consider two counterclockwise consecutive angles a, a' around a vertex (or a face). Property EDGE implies that $\ell(a') = \ell(a)$ or $\ell(a') = \ell(a) + 1$ (see Figure 6). Thus by considering all the angles around a vertex or a face, it is clear that ℓ is also VERTEX and FACE. □

Thus we define a Schnyder labeling as follows:

Definition 2.2 (Schnyder labeling) *Given a map G on an orientable surface, a* Schnyder labeling *of G is an* EDGE *angle labeling of G.*

Figure 6 shows how an EDGE angle labeling defines an orientation and coloring of the edges of the graph with edges oriented in one direction or in two opposite directions.
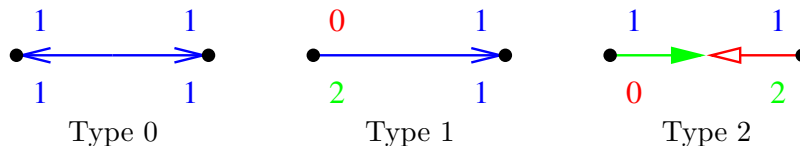

Figure 6: Correspondence between EDGE angle labelings and some bi-orientations and colorings of the edges.

In the next two sections, the correspondence from Figure 6 is used to show that Schnyder labelings correspond to or generalize previously defined Schnyder woods in the plane and in the torus. Hence, they are a natural generalization of Schnyder woods for higher genus.

2.2 Planar Schnyder woods

Originally, Schnyder woods were defined only for planar triangulations [25]. Felsner [8, 9] extended this definition to planar maps. To do so he allowed edges to be oriented in one direction or in two opposite directions (originally only one direction was possible). The formal definition is the following:

Definition 2.3 (Planar Schnyder wood) *Given a planar map G. Let x_0, x_1, x_2 be three vertices occurring in counterclockwise order on the outer face of G. The* suspension G^σ *is obtained by attaching a half-edge that reaches into the outer face to each of these special vertices. A* planar Schnyder wood *rooted at x_0, x_1, x_2 is an orientation and coloring of the edges of G^σ with the colors 0, 1, 2, where every edge e is oriented in one direction or in two opposite directions (each direction having a distinct color and being outgoing), satisfying the following conditions:*

6

- *Every vertex satisfies the Schnyder property and the half-edge at x_i is directed outward and colored i.*

- *There is no interior face whose boundary is a monochromatic cycle.*

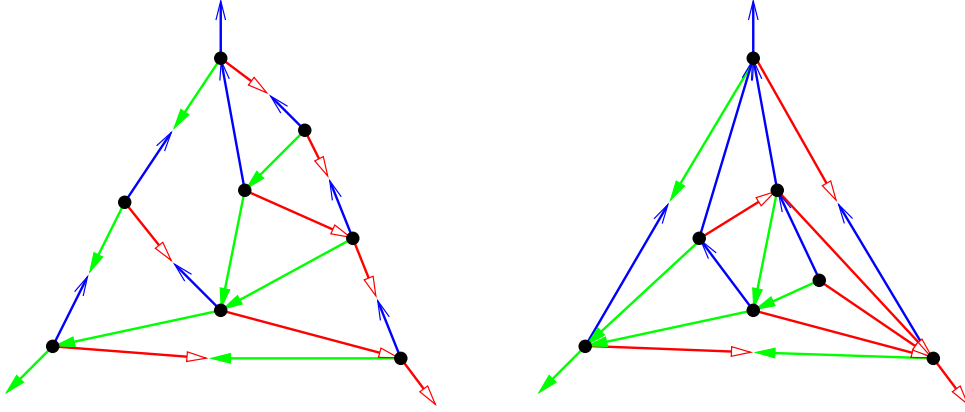See Figure 7 for two examples of planar Schnyder woods.

Figure 7: A planar Schnyder wood of a planar map and of a planar triangulation.

The correspondence of Figure 6 gives the following bijection, as proved by Felsner [9]:

Proposition 2.4 ([9]) *If G is a planar map and x_0, x_1, x_2 are three vertices occurring in counterclockwise order on the outer face of G, then the planar Schnyder woods of G^σ are in bijection with the {1,2}-EDGE, 1-VERTEX, 1-FACE angle labelings of G^σ (with the outer face being 1-FACE but in clockwise order).*

Felsner [8] and Miller [20] characterized the planar maps that admit a planar Schnyder wood. Namely, they are the internally 3-connected maps (i.e. those with three vertices on the outer face such that the graph obtained from G by adding a vertex adjacent to the three vertices is 3-connected).

2.3 Generalized Schnyder woods

Any map (on any orientable surface) admits a trivial EDGE angle labeling: the one with all angles labeled i (and thus all edges, vertices, and faces are of type 0). A natural non-trivial case, that is also symmetric for the duality, is to consider EDGE, $\mathbb{N}^*$-VERTEX, $\mathbb{N}^*$-FACE angle labelings of general maps (where $\mathbb{N}^* = \mathbb{N}\setminus\{0\}$). In planar Schnyder woods only type 1 and type 2 edges are used. Here we allow type 0 edges because they seem unavoidable for some maps (see discussion below). This suggests the following definition of Schnyder woods in higher genus.

First, the generalization of the Schnyder property is the following:

Definition 2.5 (Generalized Schnyder property) *Given a map G on a genus $g \geq 1$ orientable surface, a vertex v and an orientation and coloring of the edges incident to v with the colors 0, 1, 2, we say that v satisfies the generalized Schnyder property (see Figure 3), if v satisfies the following local property for $k \geq 1$:*

- *Vertex v has out-degree $3k$.*

- *The edges $e_0(v), \ldots, e_{3k-1}(v)$ leaving v in counterclockwise order are such that $e_j(v)$ has color j mod 3.*

- *Each edge entering v in color i enters v in a counterclockwise sector from $e_j(v)$ to $e_{j+1}(v)$ with $i \not\equiv j \pmod 3$ and $i \not\equiv j+1 \pmod 3$.*

Then, the generalization of Schnyder woods is the following (where the three types of edges depicted on Figure 6 are allowed):

Definition 2.6 (Generalized Schnyder wood) *Given a map G on a genus $g \geq 1$ orientable surface, a generalized Schnyder wood of G is an orientation and coloring of the edges of G with the colors 0, 1, 2, where every edge is oriented in one direction or in two opposite directions (each direction having a distinct color and being outgoing, or each direction having the same color and being incoming), satisfying the following conditions:*

- *Every vertex satisfies the generalized Schnyder property.*

- *There is no face whose boundary is a monochromatic cycle.*

When there is no ambiguity we call "generalized Schnyder woods" just "Schnyder woods". See Figure 8 for two examples of Schnyder woods in the torus.
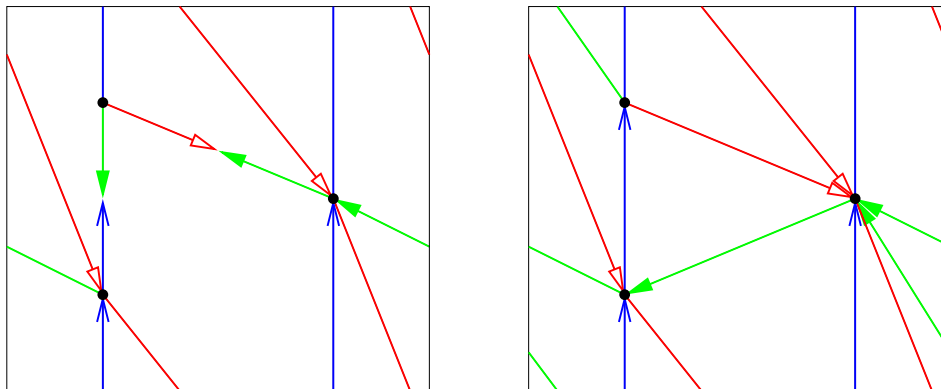

Figure 8: A Schnyder wood of a toroidal map and of a toroidal triangulation.

The first and third author already defined Schnyder woods for toroidal maps in [17]. Our definition is broader as in [17], there is also a (global) condition on the way monochromatic cycles intersect. See Section 5.2 for a discussion on this property.

Figure 4 is an example of a Schnyder wood on a triangulation of the double torus. The correspondence from Figure 6 immediately gives the following bijection whose proof is omitted.

Proposition 2.7 *If G is a map on a genus $g \geq 1$ orientable surface, then the generalized Schnyder woods of G are in bijection with the EDGE, $\mathbb{N}^*$-VERTEX, $\mathbb{N}^*$-FACE angle labelings of G.*

The examples in Figures 8 and 4 do not have type 0 edges. However, for all $g \geq 2$, there are genus g maps, with vertex degrees and face degrees at most five. Figure 9 depicts how to construct such maps, for all $g \geq 2$. For these maps, type 0 edges are unavoidable. Indeed, take such a map with an angle labeling that has only type 1 and type 2 edges. Around a type 1 or type 2 edge there are exactly three changes of labels, so in total there are exactly $3m$ such changes. As vertices and faces have degree at most five, they are either of type 0 or 1, hence the number of label changes should be at most $3n + 3f$. Thus, $3m \leq 3n + 3f$, which contradicts Euler's formula for $g \geq 2$. Furthermore, note that the maps described in Figure 9, as well as their dual maps, are 3-connected. Actually they can be modified to be 4-connected and of arbitrary large face-width.
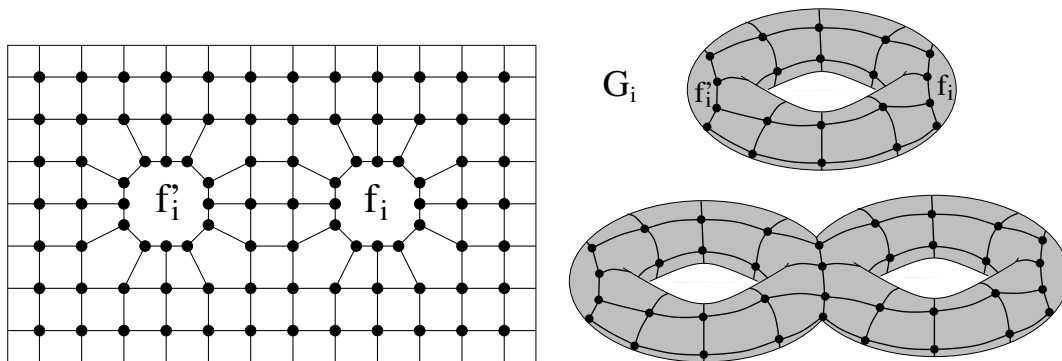
Figure 9: A toroidal map G_i with two distinguished faces, f_i and f_i'. Take g copies G_i with $1 \leq i \leq g$ and glue them by identifying f_i and f_{i+1}' for all $1 \leq i < g$. Faces f_1 and f_g' are filled to have only vertices and faces of degree at most five.

An orientation and coloring of the edges corresponding to an EDGE, $\mathbb{N}^*$-VERTEX, $\mathbb{N}^*$-FACE angle labelings is given for the double-toroidal map of Figure 10. It contains two edges of type 0 and it is 1-VERTEX and 1-FACE. Similarly, one can obtain EDGE, $\mathbb{N}^*$-VERTEX, $\mathbb{N}^*$-FACE angle labelings for any map in Figure 9.

2.4 Schnyder woods in the universal cover

In this section we prove some properties of Schnyder woods in the universal cover. We refer to [19] for the general theory of universal covers. The *universal cover* of the torus (resp. an orientable surface of genus $g \geq 2$) is a surjective mapping p from the plane
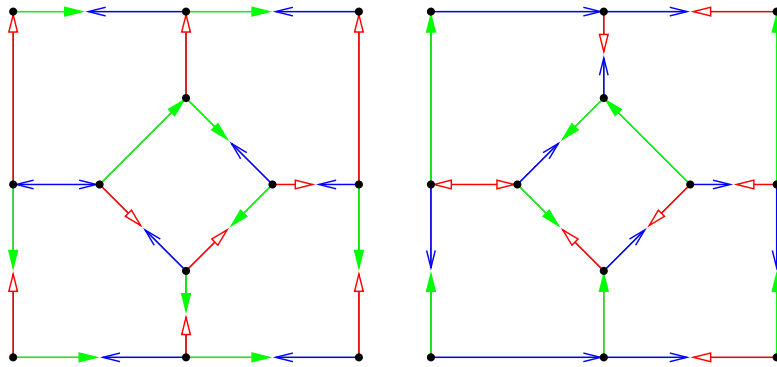
Figure 10: An orientation and coloring of the edges of a double-toroidal map that correspond to an EDGE, ℕ*-VERTEX, ℕ*-FACE angle labeling. Here, the two parts are toroidal and the two central faces are identified (by preserving the colors) to obtain a doubletoroidal map.

(resp. the open unit disk) to the surface that is locally a homeomorphism. The universal cover of the torus is obtained by replicating a flat representation of the torus to tile the plane. Figure 11 shows how to obtain the universal cover of the double torus. The key property is that a closed curve on the surface corresponds to a closed curve in the universal cover if and only if it is contractible.
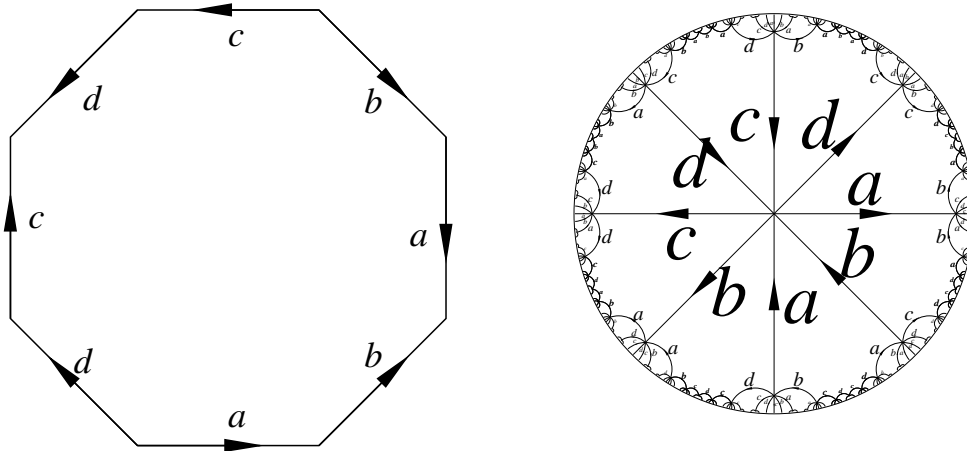
Figure 11: Canonical representation and universal cover of the double torus (source : Yann Ollivier http://www.yann-ollivier.org/maths/primer.php).

Universal covers can be used to represent a map on an orientable surface as an infinite planar map. Any property of the map can be lifted to its universal cover, as long as it is defined locally. Thus universal covers are an interesting tool for the study of Schnyder labelings since all the definitions we have given so far are purely local.

10

Consider a map G on a genus $g \geq 1$ orientable surface. Let G^∞ be the infinite planar map drawn on the universal cover and defined by $p^{-1}(G)$.

We need the following general lemma concerning universal covers:

Lemma 2.8 *Suppose that for a finite set of vertices X of G^∞, the graph $G^\infty \setminus X$ is not connected. Then $G^\infty \setminus X$ has a finite connected component.*

Proof. Suppose the lemma is false and $G^\infty \setminus X$ is not connected and has no finite component. Then it has a face bounded by an infinite number of vertices. As G is finite, the vertices of G^∞ have bounded degree. Putting back the vertices of X, a face bounded by an infinite number of vertices would remain. The border of this face does not correspond to a contractible cycle of G, a contradiction with G being a map. $\square$

Recall that a graph is *k-connected* if it has at least $k+1$ vertices and if it remains connected after removing any $k-1$ vertices. Extending the notion of essentially 2-connectedness defined in [21] for the toroidal case, we say that G is *essentially k-connected* if G^∞ is k-connected. Note that the notion of being essentially k-connected is different from G being k-connected. There is no implications in any direction. But note that since G is a map, it is essentially 1-connected.

Suppose now that G is given with a Schnyder wood (i.e. an EDGE, $\mathbb{N}^*$-VERTEX, $\mathbb{N}^*$-FACE angle labeling by Proposition 2.7). Consider the orientation and coloring of the edges of G^∞ corresponding to the Schnyder wood of G.

Let G_i^∞ be the directed graph induced by the edges of color i of G^∞. This definition includes edges that are half-colored i, and in this case, the edges get only the direction corresponding to color i. The graph $(G_i^\infty)^{-1}$ is the graph obtained from G_i^∞ by reversing all its edges. The graph $G_i^\infty \cup (G_{i-1}^\infty)^{-1} \cup (G_{i+1}^\infty)^{-1}$ is obtained from the graph G by orienting edges in one or two directions depending on whether this orientation is present in G_i^∞, $(G_{i-1}^\infty)^{-1}$ or $(G_{i+1}^\infty)^{-1}$. Similarly to what happens for planar Schnyder woods, we have the following:

Lemma 2.9 *The graph $G_i^\infty \cup (G_{i-1}^\infty)^{-1} \cup (G_{i+1}^\infty)^{-1}$ does not contain directed cycle.*

Proof. Suppose there is a directed cycle in $G_i^\infty \cup (G_{i-1}^\infty)^{-1} \cup (G_{i+1}^\infty)^{-1}$. Let C be such a cycle containing the minimum number of faces in the map D with border C. Suppose by symmetry that C turns around D counterclockwisely. Every vertex of D has at least one outgoing edge of color $i+1$ in D. So there is a cycle of color $(i+1)$ in D and this cycle is C by minimality of C. Every vertex of D has at least one outgoing edge of color i in D. So, again by minimality of C, the cycle C is a cycle of color i. Thus all the edges of C are oriented in color i counterclockwisely and in color $i+1$ clockwisely.

By the definition of Schnyder woods, there is no face the boundary of which is a monochromatic cycle, so D is not a face. Let vx be an edge in the interior of D that is outgoing for v. The vertex v can be either in the interior of D or in C (if v has more

than three outgoing arcs). In both cases, v has necessarily an edge e_i of color i and an edge e_{i+1} of color $i+1$, leaving v and in the interior of D. Consider $W_i(v)$ (resp. $W_{i+1}(v)$) a monochromatic walk starting from e_i (resp. e_{i+1}), obtained by following outgoing edges of color i (resp. $i+1$). By minimality of C those walks are not contained in D. We hence have that $W_i(v) \setminus v$ and $W_{i+1}(v) \setminus v$ intersect C. Thus each of these walks contains a non-empty subpath from v to C. The union of these two paths, plus a part of C contradicts the minimality of C. $\qquad \square$

Let v be a vertex of G^∞. For each color i, vertex v is the starting vertex of some walks of color i, we denote the union of these walks by $P_i(v)$. Every vertex has at least one outgoing edge of color i and the set $P_i(v)$ is obtained by following all these edges of color i starting from v. Note that for some vertices v, $P_i(v)$ may consist of a single walk. It is the case when v cannot reach a vertex of outdegree six or more.

Lemma 2.10 *For every vertex v and color i, the two graphs $P_{i-1}(v)$ and $P_{i+1}(v)$ intersect only on v.*

Proof. If $P_{i-1}(v)$ and $P_{i+1}(v)$ intersect on two vertices, then $G^\infty_{i-1} \cup (G^\infty_{i+1})^{-1}$ contains a cycle, contradicting Lemma 2.9. $\qquad \square$

Now we can prove the following:

Theorem 2.11 *If a map G on a genus $g \geq 1$ orientable surface admits an EDGE, $\mathbb{N}^*$-VERTEX, $\mathbb{N}^*$-FACE angle labeling, then G is essentially 3-connected.*

Proof. Towards a contradiction, suppose that there exist two vertices x, y of G^∞ such that $G' = G^\infty \setminus \{x, y\}$ is not connected. Then, by Lemma 2.8, the graph G' has a finite connected component R. Let v be a vertex of R. By Lemma 2.9, for $0 \leq i \leq 2$, the graph $P_i(v)$ does not lie in R so it intersects either x or y. So for two distinct colors i, j, the two graphs $P_i(v)$ and $P_j(v)$ intersect in a vertex distinct from v, a contradiction to Lemma 2.10. $\qquad \square$

2.5 Conjectures on the existence of Schnyder woods

Proving that every triangulation on a genus $g \geq 1$ orientable surface admits a 1-EDGE angle labeling would imply the following theorem of Barát and Thomassen [2]:

Theorem 2.12 ([2]) *A simple triangulation on a genus $g \geq 1$ orientable surface admits an orientation of its edges such that every vertex has outdegree divisible by three.*

Recently, Theorem 2.12 has been improved by Albar, the first author, and the second author [1]:

Theorem 2.13 ([1]) *A simple triangulation on a genus $g \geq 1$ orientable surface admits an orientation of its edges such that every vertex has outdegree at least three, and divisible by three.*

Note that Theorems 2.12 and 2.13 are proved only in the case of simple triangulations (i.e. no loops and no multiple edges). We believe them to be true also for non-simple triangulations without contractible loops nor contractible double edges.

Theorem 2.13 suggests the existence of 1-EDGE angle labelings with no sinks, i.e. 1-EDGE, $\mathbb{N}^*$-VERTEX angle labelings. One can easily check that in a triangulation, a 1-EDGE angle labeling is also 1-FACE. Thus we can hope that a triangulation on a genus $g \geq 1$ orientable surface admits a 1-EDGE, $\mathbb{N}^*$-VERTEX, 1-FACE angle labeling. Note that a 1-EDGE, 1-FACE angle labeling of a map implies that faces are triangles. So we propose the following conjecture, whose "only if" part follows from the previous sentence:

Conjecture 2.14 *A map on a genus $g \geq 1$ orientable surface admits a 1-EDGE, $\mathbb{N}^*$-VERTEX, 1-FACE angle labeling if and only if it is a triangulation.*

If true, Conjecture 2.14 would strengthen Theorem 2.13 in two ways. First, it considers more triangulations (not only simple ones). Second, it requires the coloring property around vertices.

How about general maps? We propose the following conjecture, whose "only if" part is Theorem 2.11:

Conjecture 2.15 *A map on a genus $g \geq 1$ orientable surface admits an EDGE, $\mathbb{N}^*$-VERTEX, $\mathbb{N}^*$-FACE angle labeling if and only if it is essentially 3-connected.*

Conjecture 2.15 implies Conjecture 2.14 since for a triangulation every face would be of type 1, and thus every edge would be of type 1. Conjecture 2.15 is proved in [17] for $g = 1$ whereas both conjectures are open for $g \geq 2$. Section 5 gives a new proof of Conjecture 2.14 for $g = 1$ based on the results in Section 3.

3   Characterization of Schnyder orientations

3.1   A bit of homology

In the next sections, we need a bit of surface homology of general maps, which we will discuss now. For a deeper introduction to homology we refer to [15].

For the sake of generality, in this subsection we consider that maps may have contractible cycles of size 1 or 2. Consider a map $G = (V, E)$, on an orientable surface of genus g, given with an arbitrary orientation of its edges. This fixed arbitrary orientation is implicit in all the paper and is used to handle flows. A *flow* ϕ on G is a vector in $\mathbb{Z}^E$. For any $e \in E$, we denote by ϕ_e the coordinate e of ϕ.

A *walk* W of G is a sequence of edges with a direction of traversal such that the ending point of an edge is the starting point of the next edge. A walk is *closed* if the start and end vertices coincide. A walk has a *characteristic flow* $\phi(W)$ defined by:

$$\phi(W)_e := \#\text{times } W \text{ traverses } e \text{ forward} - \#\text{times } W \text{ traverses } e \text{ backward}$$

This definition naturally extends to sets of walks. From now on we consider that a set of walks and its characteristic flow are the same object and by abuse of notation we can write W instead of $\phi(W)$. We do the same for *oriented subgraphs*, i.e., subgraphs that can be seen as a set of walks of unit length.

A *facial walk* is a closed walk bounding a face. Let $\mathcal{F}$ be the set of counterclockwise facial walks and let $\mathbb{F} = <\phi(\mathcal{F})>$ be the subgroup of $\mathbb{Z}^E$ generated by $\mathcal{F}$. Two flows ϕ, ϕ' are *homologous* if $\phi - \phi' \in \mathbb{F}$. They are *weakly homologous* if $\phi - \phi' \in \mathbb{F}$ or $\phi + \phi' \in \mathbb{F}$. We say that a flow ϕ is 0-homologous if it is homologous to the zero flow, i.e. $\phi \in \mathbb{F}$.

Let $\mathcal{W}$ be the set of *closed* walks and let $\mathbb{W} = <\phi(\mathcal{W})>$ be the subgroup of $\mathbb{Z}^E$ generated by $\mathcal{W}$. The group $H(G) = \mathbb{W}/\mathbb{F}$ is the *first homology group* of G. It is well-known that $H(G)$ only depends on the genus of the map, and actually it is isomorphic to $\mathbb{Z}^{2g}$.

A set $\{B_1, \ldots, B_{2g}\}$ of (closed) walks of G is said to be a *basis for the homology* if the equivalence classes of their characteristic vectors $([\phi(B_1)], \ldots, [\phi(B_{2g})])$ generate $H(G)$. Then for any closed walk W of G, we have $W = \sum_{F \in \mathcal{F}} \lambda_F F + \sum_{1 \leq i \leq 2g} \mu_i B_i$ for some $\lambda \in \mathbb{Z}^{\mathcal{F}}, \mu \in \mathbb{Z}^{2g}$. Moreover one of the λ_F can be set to zero (and then all the other coefficients are unique). Indeed, for any map, there exists a set of cycles that forms a basis for the homology and it is computationally easy to build. A possible way is by considering a spanning tree T of G, and a spanning tree T^* of G^* that contains no edges dual to T. By Euler's formula, there are exactly $2g$ edges in G that are not in T nor dual to edges of T^*. Each of these $2g$ edges forms a unique cycle with T. It is not hard to see that this set of cycles forms a basis for the homology.

The edges of the dual G^* of G are oriented such that the dual e^* of an edge e of G goes from the face on the right of e to the face on the left of e. Let $\mathcal{F}^*$ be the set of counterclockwise facial walks of G^*. Consider $\{B_1^*, \ldots, B_{2g}^*\}$ a set of closed walks of G^* that form a basis for the homology. Let p and d be flows of G and G^*, respectively. We define the following:

$$\beta(p, d) = \sum_{e \in G} p_e d_{e^*}$$

Note that β is a bilinear function.

Lemma 3.1 *Given two flows ϕ, ϕ' of G, the following properties are equivalent to each other:*

1. *The two flows ϕ, ϕ' are homologous.*

2. *For any closed walk W of G^* we have $\beta(\phi, W) = \beta(\phi', W)$.*

3. *For any $F \in \mathcal{F}^*$, we have $\beta(\phi, F) = \beta(\phi', F)$, and, for any $1 \leq i \leq 2g$, we have $\beta(\phi, B_i^*) = \beta(\phi', B_i^*)$.*

Proof. (1. $\Longrightarrow$ 3.) Suppose that ϕ, ϕ' are homologous. Then we have $\phi - \phi' = \sum_{F \in \mathcal{F}} \lambda_F F$ for some $\lambda \in \mathbb{Z}^{\mathcal{F}}$. It is easy to see that, for any closed walk W of G^*, a facial walk $F \in \mathcal{F}$ satisfies $\beta(F, W) = 0$, so $\beta(\phi, W) = \beta(\phi', W)$ by linearity of β.

(3. $\Longrightarrow$ 2.) Suppose that for any $F \in \mathcal{F}^*$, we have $\beta(\phi, F) = \beta(\phi', F)$, and, for any $1 \leq i \leq 2g$, we have $\beta(\phi, B_i^*) = \beta(\phi', B_i^*)$. Let W be any closed walk of G^*. We have $W = \sum_{F \in \mathcal{F}^*} \lambda_F F + \sum_{1 \leq i \leq 2g} \mu_i B_i^*$ for some $\lambda \in \mathbb{Z}^{\mathcal{F}}, \mu \in \mathbb{Z}^{2g}$. Then by linearity of β we have $\beta(\phi, W) = \beta(\phi', W)$.

(2. $\Longrightarrow$ 1.) Suppose $\beta(\phi, W) = \beta(\phi', W)$ for any closed walk W of G^*. Let $z = \phi - \phi'$. Thus $\beta(z, W) = 0$ for any closed walk W of G^*. We label the faces of G with elements of $\mathbb{Z}$ as follows. Choose an arbitrary face F_0 and label it 0. Then, consider any face F of G and a path P_F of G^* from F_0 to F. Label F with $\ell_F = \beta(z, P_F)$. Note that the label of F is independent from the choice of P_F. Indeed, for any two paths P_1, P_2 from F_0 to F, we have $P_1 - P_2$ is a closed walk, so $\beta(z, P_1 - P_2) = 0$ and thus $\beta(z, P_1) = \beta(z, P_2)$. Let us show that $z = \sum_{F \in \mathcal{F}} \ell_F \phi(F)$.

$$
\begin{aligned}
\sum_{F \in \mathcal{F}} \ell_F \phi(F) &= \sum_{e \in G} (\ell_{F_2} - \ell_{F_1}) \phi(e) && \text{(face } F_2 \text{ is on the left of } e \text{ and } F_1 \text{ on the right)} \\
&= \sum_{e \in G} (\beta(z, P_{F_2}) - \beta(z, P_{F_1})) \phi(e) && \text{(definition of } \ell_F) \\
&= \sum_{e \in G} \beta(z, P_{F_2} - P_{F_1}) \phi(e) && \text{(linearity of } \beta) \\
&= \sum_{e \in G} \beta(z, e^*) \phi(e) && (P_{F_1} + e^* - P_{F_2} \text{ is a closed walk}) \\
&= \sum_{e \in G} \left(\sum_{e' \in G} z_{e'} \phi(e^*)_{e'^*} \right) \phi(e) && \text{(definition of } \beta) \\
&= \sum_{e \in G} z_e \phi(e) \\
&= z
\end{aligned}
$$

So $z \in \mathbb{F}$ and thus ϕ, ϕ' are homologous. $\qquad \square$

3.2 General characterization

Consider a map G on an orientable surface of genus g. The mapping of Figure 6 shows how an EDGE angle labeling of G can be mapped to an orientation of the edges with

edges oriented in one direction or in two opposite directions. These edges can be defined more naturally in the primal-dual-completion of G.

The *primal-dual-completion* $\hat{G}$ is the map obtained from simultaneously embedding G and G^* such that vertices of G^* are embedded inside faces of G and vice-versa. Moreover, each edge crosses its dual edge in exactly one point in its interior, which also becomes a vertex of $\hat{G}$. Hence, $\hat{G}$ is a bipartite graph with one part consisting of *primal-vertices* and *dual-vertices* and the other part consisting of *edge-vertices* (of degree four). Each face of $\hat{G}$ is a quadrangle incident to one primal-vertex, one dual-vertex and two edge-vertices. Actually, the faces of $\hat{G}$ are in correspondance with the angles of G. This means that angle labelings of G correspond to face labelings of $\hat{G}$.

Given $\alpha : V \to \mathbb{N}$, an orientation of G is an α-*orientation* [10] if for every vertex $v \in V$ its outdegree $d^+(v)$ equals $\alpha(v)$. We call an orientation of $\hat{G}$ a mod_3-*orientation* if it is an α-orientation for a function α satisfying :

$$\alpha(v) \equiv \begin{cases} 0 \ (\mathrm{mod}\,3) & \text{if } v \text{ is a primal- or dual-vertex,} \\ 1 \ (\mathrm{mod}\,3) & \text{if } v \text{ is an edge-vertex.} \end{cases}$$

Note that an EDGE angle labeling of G corresponds to a mod_3-orientation of $\hat{G}$, by the mapping of Figure 12, where the three types of edges are represented. Type 0 corresponds to an edge-vertex of outdegree four. Type 1 and type 2 both correspond to an edge-vertex of outdegree 1; in type 1 (resp. type 2) the outgoing edge goes to a primal-vertex (resp. dual-vertex). In all cases we have $d^+(v) \equiv 1 \ (\mathrm{mod}\,3)$ if v is an edge-vertex. By Lemma 2.1, the labeling is also VERTEX and FACE. Thus, $d^+(v) \equiv 0 \ (\mathrm{mod}\,3)$ if v is a primal- or dual-vertex.

Type 0 Type 1 Type 2
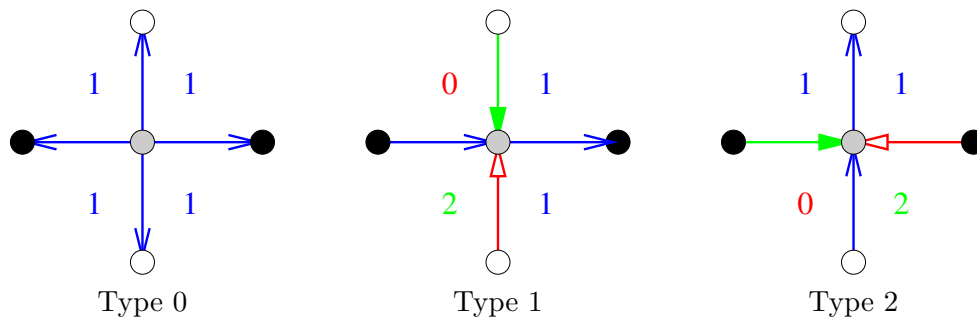
Figure 12: How to map an EDGE angle labeling to a $\mathrm{mod}\ _3$-orientation of the primal-dual completion. Primal-vertices are black, dual-vertices are white and edge-vertices are gray. This serves as a convention for the other figures.

As mentioned earlier, De Fraysseix and Ossona de Mendez [14] give a bijection between internal 3-orientations and Schnyder woods of planar triangulations. Felsner [10] generalizes this result for planar Schnyder woods and orientations of the primal-dual completion having prescribed out-degrees. The situation is more complicated in higher genus (see Figure 5). It is not enough to prescribe outdegrees in order to characterize orientations corresponding to EDGE angle labelings.

16

We call an orientation of $\hat{G}$ corresponding to an EDGE angle labeling of G a *Schnyder orientation*. In this section we characterize which orientations of $\hat{G}$ are Schnyder orientations.

Consider an orientation of the primal-dual completion $\hat{G}$. Let $Out = \{(u,v) \in E(\hat{G}) \mid v$ is an edge-vertex$\}$, i.e. the set of edges of $\hat{G}$ which are going from a primal- or dual-vertex to an edge-vertex. We call these edges *out-edges*. For ϕ a flow of the dual of the primal-dual completion $\hat{G}^*$, we define $\delta(\phi) = \beta(Out, \phi)$. More intuitively, if W is a walk of $\hat{G}^*$, then:

$$\delta(W) = \quad \#\text{out-edges crossing } W \text{ from left to right}$$
$$-\#\text{out-edges crossing } W \text{ from right to left}.$$

The bilinearity of β implies the linearity of δ. The following lemma gives a necessary and sufficient condition for an orientation to be a Schnyder orientation.

Lemma 3.2 *An orientation of $\hat{G}$ is a Schnyder orientation if and only if any closed walk W of $\hat{G}^*$ satisfies $\delta(W) \equiv 0 \pmod{3}$.*

Proof. ($\Longrightarrow$) Consider an EDGE angle labeling ℓ of G and the corresponding Schnyder orientation (see Figure 12). Figure 13 illustrates how δ counts the variation of the label when going from one face of $\hat{G}$ to another face of $\hat{G}$. The represented cases correspond to a walk W of $\hat{G}^*$ consisting of just one edge. If the edge of $\hat{G}$ crossed by W is not an out-edge, then the two labels in the face are the same and $\delta(W) = 0$. If the edge crossed by W is an out-edge, then the labels differ by one. If W is going counterclockwise around a primal- or dual-vertex, then the label increases by 1 (mod 3) and $\delta(W) = 1$. If W is going clockwise around a primal- or dual-vertex then the label decreases by 1 (mod 3) and $\delta(W) = -1$. One can check that this is consistent with all the edges depicted in Figure 12. Thus for any walk W of $\hat{G}^*$ from a face F to a face F', the value of $\delta(W) \pmod{3}$ is equal to $\ell(F') - \ell(F) \pmod{3}$. Thus if W is a closed walk then $\delta(W) \equiv 0 \pmod{3}$.

($\Longleftarrow$) Consider an orientation of $\hat{G}$ such that any closed walk W of $\hat{G}^*$ satisfies $\delta(W) \equiv 0 \pmod{3}$. Pick any face F_0 of $\hat{G}$ and label it 0. Consider any face F of $\hat{G}$ and a path P of $\hat{G}^*$ from F_0 to F. Label F with the value $\delta(P)$ mod 3. Note that the label of F is independent from the choice of P as for any two paths P_1, P_2 going from F_0 to F, we have $\delta(P_1) \equiv \delta(P_2) \pmod{3}$ since $\delta(P_1 - P_2) \equiv 0 \pmod{3}$ as $P_1 - P_2$ is a closed walk.

Consider an edge-vertex v of $\hat{G}$ and a walk W of $\hat{G}^*$ going clockwise around v. By assumption $\delta(W) \equiv 0 \pmod{3}$ and $d(v) = 4$ so $d^+(v) \equiv 1 \pmod{3}$. One can check (see Figure 12) that around an edge-vertex v of outdegree four, all the labels are the same and thus v corresponds to an edge of G of type 0. One can also check that around an edge-vertex v of outdegree 1, the labels are in clockwise order, $i-1, i, i, i+1$ for some i in $\{0, 1, 2\}$ where the two faces with the same label are incident to the outgoing edge of v. Thus, v corresponds to an edge of G of type 1 or 2 depending on the outgoing
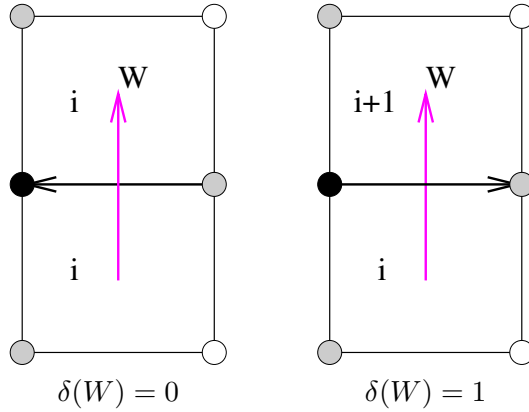
17

Figure 13: How δ counts the variation of the labels.

edge reaching a primal- or a dual-vertex. So the obtained labeling of the faces of $\hat{G}$ corresponds to an EDGE angle labeling of G and the considered orientation is a Schnyder orientation. $\qquad\square$

We now study properties of δ w.r.t homology in order to simplify the condition of Lemma 3.2. Let $\hat{\mathcal{F}}^*$ be the set of counterclockwise facial walks of $\hat{G}^*$.

Lemma 3.3 *In a* mod_3-*orientation of* $\hat{G}$, *any* $F \in \hat{\mathcal{F}}^*$ *satisfies* $\delta(F) \equiv 0 \ (\mathrm{mod}3)$.

Proof. If F corresponds to an edge-vertex v of $\hat{G}$, then v has degree exactly four and outdegree one or four by definition of mod_3-orientations. So there are exactly zero or three out-edges crossing F from right to left, and $\delta(F) \equiv 0 \ (\mathrm{mod}3)$.

If F corresponds to a primal- or dual-vertex v, then v has outdegree $0 \ (\mathrm{mod}3)$ by definition of mod_3-orientations. So there are exactly $0 \ (\mathrm{mod}3)$ out-edges crossing F from left to right, and $\delta(F) \equiv 0 \ (\mathrm{mod}3)$. $\qquad\square$

Lemma 3.4 *In a* mod_3-*orientation of* $\hat{G}$, *if* $\{B_1, \ldots, B_{2g}\}$ *is a set of cycles of* $\hat{G}^*$ *that forms a basis for the homology, then for any closed walk* W *of* $\hat{G}^*$ *homologous to* $\mu_1 B_1 + \cdots + \mu_{2g} B_{2g}$, *we have* $\delta(W) \equiv \mu_1 \delta(B_1) + \cdots + \mu_{2g} \delta(B_{2g}) \ (\mathrm{mod}3)$.

Proof. We have $W = \sum_{F \in \hat{\mathcal{F}}^*} \lambda_F F + \sum_{1 \leq i \leq 2g} \mu_i B_i$ for some $\lambda \in \mathbb{Z}^{\mathcal{F}}$. Then by linearity of δ and Lemma 3.3, the claim follows. $\qquad\square$

Lemma 3.4 can be used to simplify the condition of Lemma 3.2 and show that if $\{B_1, \ldots, B_{2g}\}$ is a set of cycles of $\hat{G}^*$ that forms a basis for the homology, then an orientation of $\hat{G}$ is a Schnyder orientation if and only if it is a mod_3-orientation such that $\delta(B_i) \equiv 0 \ (\mathrm{mod}\,3)$, for all $1 \leq i \leq 2g$. Now, we define a new function γ that is used to formulate a similar characterization theorem (see Theorem 3.7).

Consider a (not necessarily directed) cycle C of G together with a direction of traversal. We associate to C its corresponding cycle in $\hat{G}$ denoted by $\hat{C}$. We define $\gamma(C)$ by:

$$\gamma(C) = \text{\# edges of } \hat{G} \text{ leaving } \hat{C} \text{ on its right} - \text{\# edges of } \hat{G} \text{ leaving } \hat{C} \text{ on its left}$$

Since it considers cycles of $\hat{G}$ instead of walks of $\hat{G}^*$, it is easier to deal with parameter γ rather than parameter δ. However γ does not enjoy the same property w.r.t. homology as δ. For homology we have to consider walks as flows, but two walks going several time through a given vertex may have the same characteristic flow but different γ. This explains why δ is defined first. Now we adapt the results for γ.

The value of γ is related to δ by the next lemmas. Let C be a cycle of G with a direction of traversal. Let $W_L(C)$ be the closed walk of $\hat{G}^*$ just on the left of C and going in the same direction as C (i.e. $W_L(C)$ is composed of the dual edges of the edges of $\hat{G}$ incident to the left of $\hat{C}$). Note that since the faces of $\hat{G}^*$ have exactly one incident vertex that is a primal-vertex, walk $W_L(C)$ is in fact a cycle of $\hat{G}^*$. Similarly, let $W_R(C)$ be the cycle of $\hat{G}^*$ just on the right of C.

Lemma 3.5 *Consider an orientation of $\hat{G}$ and a cycle C of G, then $\gamma(C) = \delta(W_L(C)) + \delta(W_R(C))$.*

Proof. We consider the different cases that can occur. An edge that is entering a primal-vertex of $\hat{C}$, is not counting in either $\gamma(C), \delta(W_L(C)), \delta(W_R(C))$. An edge that is leaving a primal-vertex of $\hat{C}$ from its right side (resp. left side) is counting $+1$ (resp. -1) for $\gamma(C)$ and $\delta(W_R(C))$ (resp. $\delta(W_L(C))$).

For edges incident to edge-vertices of $\hat{C}$ both sides have to be considered at the same time. Let v be an edge-vertex of $\hat{C}$. Vertex v is of degree four so it has exactly two edges incident to $\hat{C}$ and not on C. One of these edges, e_L, is on the left side of $\hat{C}$ and dual to an edge of $W_L(C)$. The other edge, e_R, is on the right side of $\hat{C}$ and dual to an edge of $W_R(C)$. If e_L and e_R are both incoming edges for v, then e_R (resp. e_L) is counting -1 (resp. $+1$) for $\delta(W_R(C))$ (resp. $\delta(W_L(C))$) and not counting for $\gamma(C)$. If e_L and e_R are both outgoing edges for v, then e_R and e_L are not counting for both $\delta(W_R(C))$, $\delta(W_L(C))$ and sums to zero for $\gamma(C)$. If e_L is incoming and e_R is outgoing for v, then e_R (resp. e_L) is counting 0 (resp. $+1$) for $\delta(W_R(C))$ (resp. $\delta(W_L(C))$), and counting $+1$ (resp. 0) for $\gamma(C)$. The last case, e_L is outgoing and e_R is incoming, is symmetric and one can see that in the four cases we have that e_L and e_R count the same for $\gamma(C)$ and $\delta(W_L(C)) + \delta(W_R(C))$. We conclude $\gamma(C) = \delta(W_L(C)) + \delta(W_R(C))$. $\square$

Lemma 3.6 *In a mod_3-orientation of G, a cycle C of G satisfies*

$$\delta(W_L(C)) \equiv 0 \ (\mathrm{mod}3) \quad and \quad \delta(W_R(C)) \equiv 0 \ (\mathrm{mod}3) \iff \gamma(C) \equiv 0 \ (\mathrm{mod}3)$$

Proof. ($\implies$) Clear by Lemma 3.5.

($\Longleftarrow$) Suppose that $\gamma(C) \equiv 0 \pmod 3$. Let x_L (resp. y_L) be the number of edges of $\hat{G}$ that are dual to edges of $W_L(C)$, that are outgoing for a primal-vertex of $\hat{C}$ (resp. incoming for an edge-vertex of $\hat{C}$). Similarly, let x_R (resp. y_R) be the number of edges of $\hat{G}$ that are dual to edges of $W_R(C)$, that are outgoing for a primal-vertex of $\hat{C}$ (resp. incoming for an edge-vertex of $\hat{C}$). So $\delta(W_L(C)) = y_L - x_L$ and $\delta(W_R(C)) = x_R - y_R$. So by Lemma 3.5, $\gamma(C) = \delta(W_L(C)) + \delta(W_R(C)) = (y_L + x_R) - (x_L + y_R) \equiv 0 \pmod 3$.

Let k be the number of vertices of C. So $\hat{C}$ has k primal-vertices, k edge-vertices and $2k$ edges. Edge-vertices have outdegree 1 ($\mod 3$) so their total number of outgoing edges on $\hat{C}$ is $k + (y_L + y_R) \pmod 3$. Primal-vertices have outdegree 0 $\pmod 3$ so their total number of outgoing edges on $\hat{C}$ is $-(x_L + x_R) \pmod 3$. So in total $2k \equiv k + (y_L + y_R) - (x_L + x_R) \pmod 3$. So $(y_L + y_R) - (x_L + x_R) \equiv 0 \pmod 3$. By combining this with plus (resp. minus) $(y_L + x_R) - (x_L + y_R) \equiv 0 \pmod 3$, one obtains that $2\delta(W_L(C)) = 2(y_L - x_L) \equiv 0 \pmod 3$ (resp. $2\delta(W_R(C)) = 2(x_R - y_R) \equiv 0 \pmod 3$). Since $\delta(W_L(C))$ and $\delta(W_R(C))$ are integer we obtain $\delta(W_L(C)) \equiv 0 \pmod 3$ and $\delta(W_R(C)) \equiv 0 \pmod 3$. $\square$

Finally we have the following characterization theorem concerning Schnyder orientations:

Theorem 3.7 *Consider a map G on an orientable surface of genus g. Let $\{B_1, \ldots, B_{2g}\}$ be a set of cycles of G that forms a basis for the homology. An orientation of $\hat{G}$ is a Schnyder orientation if and only if it is a mod_3-orientation such that $\gamma(B_i) \equiv 0 \pmod 3$, for all $1 \leq i \leq 2g$.*

Proof. ($\Longrightarrow$) Consider an EDGE angle labeling ℓ of G and the corresponding Schnyder orientation (see Figure 12). Type 0 edges correspond to edge-vertices of outdegree four, while type 1 and 2 edges correspond to edge-vertices of outdegree 1. Thus $d^+(v) \equiv 1 \pmod 3$ if v is an edge-vertex. By Lemma 2.1, the labeling is VERTEX and FACE. Thus $d^+(v) \equiv 0 \pmod 3$ if v is a primal- or dual-vertex. So the orientation is a mod_3-orientation. By Lemma 3.2, we have $\delta(W) \equiv 0 \pmod 3$ for any closed walk W of $\hat{G}^*$. So we have that $\delta(W_L(B_1)), \ldots, \delta(W_L(B_{2g})), \delta(W_R(B_1)), \ldots, \delta(W_R(B_{2g}))$ are all congruent to 0 $\pmod 3$. Thus, by Lemma 3.6, we have $\gamma(B_i) \equiv 0 \pmod 3$, for all $1 \leq i \leq 2g$.

($\Longleftarrow$) Consider a mod_3-orientation of G such that $\gamma(B_i) \equiv 0 \pmod 3$, for all $1 \leq i \leq 2g$. By Lemma 3.6, we have $\delta(W_L(B_i)) \equiv 0 \pmod 3$ for all $1 \leq i \leq 2g$. Moreover $\{W_L(B_1), \ldots, W_L(B_{2g})\}$ forms a basis for the homology. So by Lemma 3.4, $\delta(W) \equiv 0 \pmod 3$ for any closed walk W of $\hat{G}^*$. So the orientation is a Schnyder orientation by Lemma 3.2. $\square$

The condition of Theorem 3.7 is easy to check: choose $2g$ cycles that form a basis for the homology and check whether γ is congruent to 0 mod 3 for each of them.

When restricted to triangulations and to edges of type 1 only, the defintion of γ can be simplified. Consider a triangulation G on an orientable surface of genus g and an orientation of the edges of G. Figure 14 shows how to transform the orientation of

G into an orientation of $\hat{G}$. Note that all the edge-vertices have outdegree exactly 1. Furthermore, all the dual-vertices only have outgoing edges and since we are considering triangulations they have outdegree exactly three.
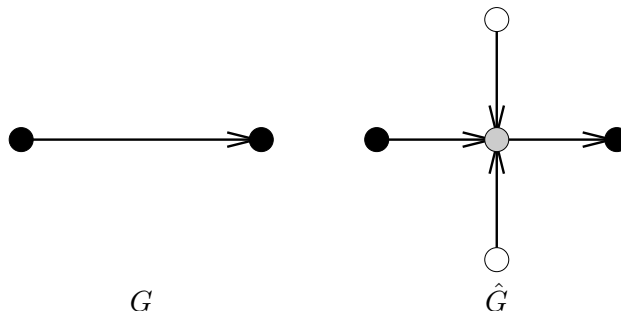

Figure 14: How to transform an orientation of a triangulation G into an orientation of $\hat{G}$.

Then the definition of γ can be simplified by the following:

$$\gamma(C) = \# \text{ edges of } G \text{ leaving } C \text{ on its right} - \# \text{ edges of } G \text{ leaving } C \text{ on its left}$$

Note that comparing to the general definition of γ, only the symbols ˆ have been removed.

The orientation of the toroidal triangulation on the left of Figure 5 is an example of a 3-orientation of a toroidal triangulation where some non contractible cycles have value γ not congruent to 0 mod 3. The value of γ for the three loops is $2, 0$ and -2. This explains why this orientation does not correspond to a Schnyder wood. On the contrary, on the right of the figure, the three loops have γ equal to 0 and we have a Schnyder wood.

4 Structure of Schnyder orientations

4.1 Transformations between Schnyder orientations

We investigate the structure of the set of Schnyder orientations of a given graph. For that purpose we need some definitions that are given on a general map G and then applied to $\hat{G}$.

Consider a map G on an orientable surface of genus g. Given two orientations D and D' of G, let $D \setminus D'$ denote the subgraph of D induced by the edges that are not oriented as in D'.

An oriented subgraph T of G is *partitionable* if its edge set can be partitioned into three sets T_0, T_1, T_2 such that all the T_i are pairwise homologous, i.e. $T_i - T_j \in \mathbb{F}$ for $i, j \in \{0, 1, 2\}$. An oriented subgraph T of G is called a *topological Tutte-orientation* if $\beta(T, W) \equiv 0 \pmod 3$ for every closed walk W in G^* (more intuitively, the number of

edges crossing W from left to right minus the number of those crossing W from right to left is divisible by three).

The name "topological Tutte-orientation" comes from the fact that an oriented graph T is called a *Tutte-orientation* if the difference of outdegree and indegree is divisible by three, i.e. $d^+(v) - d^-(v) \equiv 0 \pmod 3$, for every vertex v. So a topological Tutte-orientation is a Tutte orientation, since the latter requires the condition of the topological Tutte orientation only for the walks W of G^* going around a vertex v of G.

The notions of partitionable and topological Tutte-orientation are equivalent:

Lemma 4.1 *An oriented subgraph of G is partitionable if and only if it is a topological Tutte-orientation.*

Proof. ($\Longrightarrow$) If T is partitionable, then by definition it is the disjoint union of three homologous edge sets T_0, T_1, and T_2. Hence by Lemma 3.1, $\beta(T_0, W) = \beta(T_1, W) = \beta(T_2, W)$ for any closed walk W of G^*. By linearity of β this implies that $\beta(T, W) \equiv 0 \pmod 3$ for any closed walk W of G^*. So T is a topological Tutte-orientation.

($\Longleftarrow$) Let T be a topological Tutte-orientation of G, i.e. $\beta(T, W) \equiv 0 \pmod 3$ for any closed walk W of G^*. In the following, T-*faces* are the faces of T considered as an embedded graph. Note that T-faces are not necessarily disks. Let us introduce a $\{0, 1, 2\}$-labeling of the T-faces. Label an arbitrary T-face F_0 by 0. For any T-face F, find a path P of G^* from F_0 to F. Label F with $\beta(T, P) \pmod 3$. Note that the label of F is independent from the choice of P by our assumption on closed walks. For $0 \leq i \leq 2$, let T_i be the set of edges of T with two incident T-faces labeled $i - 1$ and $i + 1$. Note that an edge of T_i has label $i - 1$ on its left and label $i + 1$ on its right. The sets T_i form a partition of the edges of T. Let $\mathcal{F}_i$ be the counterclockwise facial walks of G that are in a T-face labeled i. We have $\phi(T_{i+1}) - \phi(T_{i-1}) = \sum_{F \in \mathcal{F}_i} \phi(F)$, so the T_i are homologous. $\square$

Let us refine the notion of partitionable. Denote by $\mathcal{E}$ the set of *oriented Eulerian subgraphs* of G (i.e. the oriented subgraphs of G where each vertex has the same in- and out-degree). Consider a partitionable oriented subgraph T of G, with edge set partition T_0, T_1, T_2 having the same homology. We say that T is *Eulerian-partitionable* if $T_i \in \mathcal{E}$ for all $0 \leq i \leq 2$. Note that if T is Eulerian-partitionable then it is Eulerian. Note that an oriented subgraph T of G that is 0-homologous is also Eulerian and thus Eulerian-partitionable (with the partition $T, \emptyset, \emptyset$).

We now investigate the structure of Schnyder orientations. For that purpose, consider a map G on an orientable surface of genus g and apply the above definitions and results to orientations of $\hat{G}$.

Let D, D' be two orientations of $\hat{G}$ such that D is a Schnyder orientation and $T = D \setminus D'$. Let $Out = \{(u, v) \in E(D) \mid v \text{ is an edge-vertex}\}$. Similarly, let $Out' = \{(u, v) \in E(D') \mid v \text{ is an edge-vertex}\}$. Note that an edge of T is either in Out or in Out', so $\phi(T) = \phi(Out) - \phi(Out')$. By Lemma 3.2, for any closed walk W of $\hat{G}^*$, $\beta(Out, W) \equiv$

$0 \pmod 3$. The three following lemmas give necessary and sufficient conditions on T for D' being a Schnyder orientation.

Lemma 4.2 D' *is a Schnyder orientation if and only if T is partitionable.*

Proof. Let D' is a Schnyder orientation. By Lemma 3.2, this is equivalent to the fact that for any closed walk W of $\hat{G}^*$, we have $\beta(Out', W) \equiv 0 \pmod 3$. Since $\beta(Out, W) \equiv 0 \pmod 3$, this is equivalent to the fact that for any closed walk W of $\hat{G}^*$, we have $\beta(T, W) \equiv 0 \pmod 3$. Finally, by Lemma 4.1 this is equivalent to T being partitionable. $\square$

Lemma 4.3 D' *is a Schnyder orientation having the same outdegrees as D if and only if T is Eulerian-partitionable.*

Proof. ($\Longrightarrow$) Suppose D' is a Schnyder orientation having the same outdegrees as D. Lemma 4.2 implies that T is partitionable into T_0, T_1, T_2 having the same homology. By Lemma 3.1, for each closed walk W of $\hat{G}^*$, we have $\beta(T_0, W) = \beta(T_1, W) = \beta(T_2, W)$. Since D, D' have the same outdegrees, we have that T is Eulerian. Consider a vertex v of $\hat{G}$ and a walk W_v of $\hat{G}^*$ going counterclockwise around v. For any oriented subgraph H of $\hat{G}^*$, we have $d_H^+(v) - d_H^-(v) = \beta(H, W_v)$, where $d_H^+(v)$ and $d_H^-(v)$ denote the outdegree and indegree of v restricted to H, respectively. Since T is Eulerian, we have $\beta(T, W_v) = 0$. Since $\beta(T_0, W_v) = \beta(T_1, W_v) = \beta(T_2, W_v)$ and $\sum \beta(T_i, W_v) = \beta(T, W_v) = 0$, we obtain that $\beta(T_0, W_v) = \beta(T_1, W_v) = \beta(T_2, W_v) = 0$. So each T_i is Eulerian.

($\Longleftarrow$) Suppose T is Eulerian-partitionable. Then Lemma 4.2 implies that D' is a Schnyder orientation. Since T is Eulerian, the two orientations D, D' have the same outdegrees. $\square$

Consider $\{B_1, \ldots, B_{2g}\}$ a set of cycles of G that forms a basis for the homology. For $\Gamma \in \mathbb{Z}^{2g}$, an orientation of $\hat{G}$ is of *type* Γ if $\gamma(B_i) = \Gamma_i$ for all $1 \leq i \leq 2g$.

Lemma 4.4 D' *is a Schnyder orientation having the same outdegrees and the same type as D (for the considered basis) if and only if T is 0-homologous (i.e. D, D' are homologous).*

Proof. ($\Longrightarrow$) Suppose D' is a Schnyder orientation having the same outdegrees and the same type as D. Then, Lemma 4.3 implies that T is Eulerian-partitionable and thus Eulerian. So for any $F \in \hat{\mathcal{F}}^*$, we have $\beta(T, F) = 0$. Moreover, for $1 \leq i \leq 2g$, consider the region R_i between $W_L(B_i)$ and $W_R(B_i)$ containing B_i. Since T is Eulerian, it is going in and out of R_i the same number of times. So $\beta(T, W_L(B_i) - W_R(B_i)) = 0$. Since D, D' have the same type, we have $\gamma_D(B_i) = \gamma_{D'}(B_i)$. So by Lemma 3.5, $\delta_D(W_L(B_i)) + \delta_D(W_R(B_i)) = \delta_{D'}(W_L(B_i)) + \delta_{D'}(W_R(B_i))$. Thus $\beta(T, W_L(B_i) + W_R(B_i)) = \beta(Out - Out', W_L(B_i) + W_R(B_i)) = \delta_D(W_L(B_i)) + \delta_D(W_R(B_i)) - \delta_{D'}(W_L(B_i)) - \delta_{D'}(W_R(B_i)) = 0$.

23

By combining this with the previous equality, we obtain $\beta(T, W_L(B_i)) = \beta(T, W_R(B_i)) = 0$ for all $1 \le i \le 2g$. Thus by Lemma 3.1, we have that T is 0-homologous.

($\Longleftarrow$) Suppose that T is 0-homologous. Then T is in particular Eulerian-partitionable (with the partition $T, \emptyset, \emptyset$). So Lemma 4.3 implies that D' is a Schnyder orientation with the same outdegrees as D. Since T is 0-homologous, by Lemma 3.1, for all $1 \le i \le 2g$, we have $\beta(T, W_L(B_i)) = \beta(T, W_R(B_i)) = 0$. Thus $\delta_D(W_L(B_i)) = \beta(Out, W_L(B_i)) = \beta(Out', W_L(B_i)) = \delta_{D'}(W_L(B_i))$ and $\delta_D(W_R(B_i)) = \beta(Out, W_R(B_i)) = \beta(Out', W_R(B_i)) = \delta_{D'}(W_R(B_i))$. So by Lemma 3.5, $\gamma_D(B_i) = \delta_D(W_L(B_i)) + \delta_D(W_R(B_i)) = \delta_{D'}(W_L(B_i)) + \delta_{D'}(W_R(B_i)) = \gamma_{D'}(B_i)$. So D, D' have the same type. $\square$

Lemma 4.4 implies that when you consider Schnyder orientations having the same outdegrees the property that they have the same type does not depend on the choice of the basis since being homologous does not depend on the basis. So we have the following:

Lemma 4.5 *If two Schnyder orientations have the same outdegrees and the same type (for the considered basis), then they have the same type for any basis.*

Lemma 4.2, 4.3 and 4.4 are summarized in the following theorem (where by Lemma 4.5 we do not have to assume a particular choice of a basis for the third item):

Theorem 4.6 *Let G be a map on an orientable surface and D, D' orientations of $\hat{G}$ such that D is a Schnyder orientation and $T = D \setminus D'$. We have the following:*

- *D' is a Schnyder orientation if and only if T is partitionable.*

- *D' is a Schnyder orientation having the same outdegrees as D if and only if T is Eulerian-partitionable.*

- *D' is a Schnyder orientation having the same outdegrees and the same type as D if and only if T is 0-homologous (i.e. D, D' are homologous).*

We show in the next section that the set of Schnyder orientations that are homologous (see third item of Theorem 4.6) carries a structure of distributive lattice.

4.2 The distributive lattice of homologous orientations

For the sake of generality, in this subsection we consider that maps may have contractible cycles of size 1 or 2. Consider a map G on an orientable surface and a given orientation D_0 of G. Let $O(G, D_0)$ be the set of all the orientations of G that are homologous to D_0. In this section we prove that $O(G, D_0)$ forms a distributive lattice. We show some additional interesting properties that are used in a recent paper by Despré, the first author, and the third author [7]. This generalizes results for the plane obtained by Ossona de Mendez [22] and Felsner [10]. The distributive lattice structure also can also

be derived from a result of Propp [24] interpreted on the dual map, see the discussion below Theorem 4.7.

In order to define an order on $O(G, D_0)$, fix an arbitrary face f_0 of G and let F_0 be its counterclockwise facial walk. Let $\mathcal{F}' = \mathcal{F} \setminus \{F_0\}$ (where $\mathcal{F}$ is the set of counterclockwise facial walks of G as defined earlier). Note that $\phi(F_0) = -\sum_{F \in \mathcal{F}'} \phi(F)$. Since the characteristic flows of $\mathcal{F}'$ are linearly independent, any oriented subgraph of G has at most one representation as a combination of characteristic flows of $\mathcal{F}'$. Moreover the 0-homologous oriented subgraphs of G are precisely the oriented subgraph that have such a representation. We say that a 0-homologous oriented subgraph T of G is *counterclockwise* (resp. *clockwise*) if its characteristic flow can be written as a combination with positive (resp. negative) coefficients of characteristic flows of $\mathcal{F}'$, i.e. $\phi(T) = \sum_{F \in \mathcal{F}'} \lambda_F \phi(F)$, with $\lambda \in \mathbb{N}^{|\mathcal{F}'|}$ (resp. $-\lambda \in \mathbb{N}^{|\mathcal{F}'|}$). Given two orientations D, D', of G we set $D \leq_{f_0} D'$ if and only if $D \setminus D'$ is counterclockwise. Then we have the following theorem.

Theorem 4.7 ([24]) *Let G be a map on an orientable surface given with a particular orientation D_0 and a particular face f_0. Let $O(G, D_0)$ the set of all the orientations of G that are homologous to D_0. We have $(O(G, D_0), \leq_{f_0})$ is a distributive lattice.*

We attribute Theorem 4.7 to Propp even if it is not presented in this form in [24]. Here we do not introduce Propp's formalism, but provide a new proof of Theorem 4.7 (as a consequence of the forthcoming Proposition 4.7). This allows us to introduce notions used later in the study of this lattice. It is notable that the study of this lattice found applications in [7], where the authors found a bijection between toroidal triangulations and unicellular toroidal maps.

To prove Theorem 4.7, we need to define the elementary flips that generates the lattice. We start by reducing the graph G. We call an edge of G *rigid with respect to* $O(G, D_0)$ if it has the same orientation in all elements of $O(G, D_0)$. Rigid edges do not play a role for the structure of $O(G, D_0)$. We delete them from G and call the obtained embedded graph $\widetilde{G}$. This graph is embedded but it is not necessarily a map, as some faces may not be homeomorphic to open disks. Note that if all the edges are rigid, i.e. $|O(G, D_0)| = 1$, then $\widetilde{G}$ has no edges.

Lemma 4.8 *Given an edge e of G, the following are equivalent:*

1. *e is non-rigid*

2. *e is contained in a 0-homologous oriented subgraph of D_0*

3. *e is contained in a 0-homologous oriented subgraph of any element of $O(G, D_0)$*

Proof. $(1 \implies 3)$ Let $D \in O(G, D_0)$. If e is non-rigid, then it has a different orientation in two elements D', D'' of $O(G, D_0)$. Then we can assume by symmetry that e has a different orientation in D and D' (otherwise in D and D'' by symmetry). Since D, D'

are homologous to D_0, they are also homologous to each other. So $T = D \setminus D'$ is a 0-homologous oriented subgraph of D that contains e.

$(3 \implies 2)$ Trivial since $D_0 \in O(G, D_0)$

$(2 \implies 1)$ If an edge e is contained in a 0-homologous oriented subgraph T of D_0. Then let D be the element of $O(G, D_0)$ such that $T = D_0 \setminus D$. Clearly e is oriented differently in D and D_0, thus it is non-rigid. $\qquad \square$

By Lemma 4.8, one can build $\widetilde{G}$ by keeping only the edges that are contained in a 0-homologous oriented subgraph of D_0. Note that this implies that all the edges of $\widetilde{G}$ are incident to two distinct faces of $\widetilde{G}$. Denote by $\widetilde{\mathcal{F}}$ the set of oriented subgraphs of $\widetilde{G}$ corresponding to the boundaries of faces of $\widetilde{G}$ considered counterclockwise. Note that any $\widetilde{F} \in \widetilde{\mathcal{F}}$ is 0-homologous and so its characteristic flows has a unique way to be written as a combination of characteristic flows of $\mathcal{F}'$. Moreover this combination can be written $\phi(\widetilde{F}) = \sum_{F \in X_{\widetilde{F}}} \phi(F)$, for $X_{\widetilde{F}} \subseteq \mathcal{F}'$. Let $\widetilde{f_0}$ be the face of $\widetilde{G}$ containing f_0 and $\widetilde{F_0}$ be the element of $\widetilde{\mathcal{F}}$ corresponding to the boundary of $\widetilde{f_0}$. Let $\widetilde{\mathcal{F}}' = \widetilde{\mathcal{F}} \setminus \{\widetilde{F_0}\}$. The elements of $\widetilde{\mathcal{F}}'$ are precisely the elementary flips which suffice to generate the entire distributive lattice $(O(G, D_0), \leq_{f_0})$.

We prove two technical lemmas concerning $\widetilde{\mathcal{F}}'$:

Lemma 4.9 *Let $D \in O(G, D_0)$ and T be a non-empty 0-homologous oriented subgraph of D. Then there exist edge-disjoint oriented subgraphs $T_1, \ldots, T_k$ of D such that $\phi(T) = \sum_{1 \leq i \leq k} \phi(T_i)$, and, for $1 \leq i \leq k$, there exists $\widetilde{X_i} \subseteq \widetilde{\mathcal{F}}'$ and $\epsilon_i \in \{-1, 1\}$ such that $\phi(T_i) = \epsilon_i \sum_{\widetilde{F} \in \widetilde{X_i}} \phi(\widetilde{F})$.*

Proof. Since T is 0-homologous, we have $\phi(T) = \sum_{F \in \mathcal{F}'} \lambda_F \phi(F)$, for $\lambda \in \mathbb{Z}^{|\mathcal{F}'|}$. Let $\lambda_{f_0} = 0$. Thus we have $\phi(T) = \sum_{F \in \mathcal{F}} \lambda_F \phi(F)$. Let $\lambda_{\min} = \min_{F \in \mathcal{F}} \lambda_F$ and $\lambda_{\max} = \max_{F \in \mathcal{F}} \lambda_F$. We may have $\lambda_{\min} = 0$ or $\lambda_{\max} = 0$ but not both since T is non-empty. For $1 \leq i \leq \lambda_{\max}$, let $X_i = \{F \in \mathcal{F}' \mid \lambda_F \geq i\}$ and $\epsilon_i = 1$. Let $X_0 = \emptyset$ and $\epsilon_0 = 1$. For $\lambda_{\min} \leq i \leq -1$, let $X_i = \{F \in \mathcal{F}' \mid \lambda_F \leq i\}$ and $\epsilon_i = -1$. For $\lambda_{\min} \leq i \leq \lambda_{\max}$, let T_i be the oriented subgraph such that $\phi(T_i) = \epsilon_i \sum_{F \in X_i} \phi(F)$. Then we have $\phi(T) = \sum_{\lambda_{\min} \leq i \leq \lambda_{\max}} \phi(T_i)$.

Since T is an oriented subgraph, we have $\phi(T) \in \{-1, 0, 1\}^{|E(G)|}$. Thus for any edge of G, incident to faces F_1 and F_2, we have $(\lambda_{F_1} - \lambda_{F_2}) \in \{-1, 0, 1\}$. So, for $1 \leq i \leq \lambda_{\max}$, the oriented graph T_i is the border between the faces with λ value equal to i and $i - 1$. Symmetrically, for $\lambda_{\min} \leq i \leq -1$, the oriented graph T_i is the border between the faces with λ value equal to i and $i + 1$. So all the T_i are edge disjoint and are oriented subgraphs of D.

Let $\widetilde{X_i} = \{\widetilde{F} \in \widetilde{\mathcal{F}}' \mid \phi(\widetilde{F}) = \sum_{F \in X'} \phi(F) \text{ for some } X' \subseteq X_i\}$. Since T_i is 0-homologous, the edges of T_i can be reversed in D to obtain another element of $O(G, D_0)$. Thus there is no rigid edge in T_i. Thus $\phi(T_i) = \epsilon_i \sum_{F \in X_i} \phi(F) = \epsilon_i \sum_{\widetilde{F} \in \widetilde{X_i}} \phi(\widetilde{F})$. $\qquad \square$

26

Lemma 4.10 *Let $D \in O(G, D_0)$ and T be a non-empty 0-homologous oriented subgraph of D such that there exists $\widetilde{X} \subseteq \widetilde{\mathcal{F}}'$ and $\epsilon \in \{-1, 1\}$ satisfying $\phi(T) = \epsilon \sum_{\widetilde{F} \in \widetilde{X}} \phi(\widetilde{F})$. Then there exists $\widetilde{F} \in \widetilde{X}$ such that $\epsilon \, \phi(\widetilde{F})$ corresponds to an oriented subgraph of D.*

Proof. The proof is done by induction on $|\widetilde{X}|$. Assume that $\epsilon = 1$ (the case $\epsilon = -1$ is proved similarly).

If $|\widetilde{X}| = 1$, then the conclusion is clear since $\phi(T) = \sum_{\widetilde{F} \in \widetilde{X}} \phi(\widetilde{F})$. We now assume that $|\widetilde{X}| > 1$. Towards a contradiction, suppose that for any $\widetilde{F} \in \widetilde{X}$ we do not have the conclusion, i.e $\phi(\widetilde{F})_e \neq \phi(T)_e$ for some $e \in \widetilde{F}$. Let $\widetilde{F_1} \in \widetilde{X}$ and $e \in \widetilde{F_1}$ such that $\phi(\widetilde{F_1})_e \neq \phi(T)_e$. Since $\widetilde{F_1}$ is counterclockwise, we have $\widetilde{F_1}$ on the left of e. Let $\widetilde{F_2} \in \widetilde{\mathcal{F}}$ that is on the right of e. Note that $\phi(\widetilde{F_1})_e = -\phi(\widetilde{F_2})_e$ and for any other face $\widetilde{F} \in \widetilde{\mathcal{F}}$, we have $\phi(\widetilde{F})_e = 0$. Since $\phi(T) = \sum_{\widetilde{F} \in \widetilde{X}} \phi(\widetilde{F})$, we have $\widetilde{F_2} \in \widetilde{X}$ and $\phi(T)_e = 0$. By possibly swapping the role of $\widetilde{F_1}$ and $\widetilde{F_2}$, we can assume that $\phi(D)_e = \phi(\widetilde{F_1})_e$, i.e., e is oriented the same way in $\widetilde{F_1}$ and D. Since e is not rigid, there exists an orientation D' in $O(G, D_0)$ such that $\phi(D)_e = -\phi(D')_e$.

Let T' be the non-empty 0-homologous oriented subgraph of D such that $T' = D \setminus D'$. Lemma 4.9 implies that there exists edge-disjoint oriented subgraphs $T_1, \ldots, T_k$ of D such that $\phi(T) = \sum_{1 \leq i \leq k} \phi(T_i)$, and, for $1 \leq i \leq k$, there exists $\widetilde{X_i} \subseteq \widetilde{\mathcal{F}}'$ and $\epsilon_i \in \{-1, 1\}$ such that $\phi(T_i) = \epsilon_i \sum_{\widetilde{F} \in \widetilde{X_i}} \phi(\widetilde{F})$. Since T' is the disjoint union of $T_1, \ldots, T_k$, there exists $1 \leq i \leq k$, such that e is an edge of T_i. Assume by symmetry that e is an edge of T_1. Since $\phi(T_1)_e = \phi(D)_e = \phi(\widetilde{F_1})_e$, we have $\epsilon_1 = 1$, $\widetilde{F_1} \in \widetilde{X_1}$ and $\widetilde{F_2} \notin \widetilde{X_1}$.

Let $\widetilde{Y} = \widetilde{X} \cap \widetilde{X_1}$. Thus $\widetilde{F_1} \in \widetilde{Y}$ and $\widetilde{F_2} \notin \widetilde{Y}$. So $|\widetilde{Y}| < |\widetilde{X}|$. Let $T_{\widetilde{Y}}$ be the oriented subgraph of G such that $T_{\widetilde{Y}} = \sum_{\widetilde{F} \in \widetilde{Y}} \phi(\widetilde{F})$. Note that the edges of T (resp. T_1) are those incident to exactly one face of $\widetilde{X}$ (resp. $\widetilde{X_1}$). Similarly every edge of $T_{\widetilde{Y}}$ is incident to exactly one face of $\widetilde{Y} = \widetilde{X} \cap \widetilde{X_1}$, i.e. it has one incident face in $\widetilde{Y} = \widetilde{X} \cap \widetilde{X_1}$ and the other incident face not in $\widetilde{X}$ or not in $\widetilde{X_1}$. In the first case this edge is in T, otherwise it is in T_1. So every edge of $T_{\widetilde{Y}}$ is an edge of $T \cup T_1$. Hence $T_{\widetilde{Y}}$ is an oriented subgraph of D. So we can apply the induction hypothesis on $T_{\widetilde{Y}}$. This implies that there exists $\widetilde{F} \in \widetilde{Y}$ such that $\widetilde{F}$ is an oriented subgraph of D. Since $\widetilde{Y} \subseteq \widetilde{X}$, this is a contradiction to our assumption. $\qquad \square$

We need the following characterization of distributive lattice from [11]:

Theorem 4.11 ([11]) *An oriented graph $\mathcal{H} = (V, E)$ is the Hasse diagram of a distributive lattice if and only if it is connected, acyclic, and admits an edge-labeling c of the edges such that:*

- *if $(u, v), (u, w) \in E$ then*

  (U1) $c(u, v) \neq c(u, w)$ and

  (U2) there is $z \in V$ such that $(v, z), (w, z) \in E$, $c(u, v) = c(w, z)$, and $c(u, w) = c(v, z)$.

- *if $(v, z), (w, z) \in E$ then*

  (L1) $c(v, z) \neq c(w, z)$ and

  (L2) there is $u \in V$ such that $(u, v), (u, w) \in E$, $c(u, v) = c(w, z)$, and $c(u, w) = c(v, z)$.

We define the directed graph $\mathcal{H}$ with vertex set $O(G, D_0)$. There is an oriented edge from D_1 to D_2 in $\mathcal{H}$ (with $D_1 \leq_{f_0} D_2$) if and only if $D_1 \setminus D_2 \in \widetilde{\mathcal{F}}'$. We define the label of that edge as $c(D_1, D_2) = D_1 \setminus D_2$. We show that $\mathcal{H}$ fulfills all the conditions of Theorem 4.11, and thus obtain the following:

Proposition 4.12 $\mathcal{H}$ *is the Hasse diagram of a distributive lattice.*

Proof. The characteristic flows of elements of $\widetilde{\mathcal{F}}'$ form an independent set, hence the digraph $\mathcal{H}$ is acyclic. By definition all outgoing and all incoming edges of a vertex of $\mathcal{H}$ have different labels, i.e. the labeling c satisfies (U1) and (L1). If (D_u, D_v) and (D_u, D_w) belong to $\mathcal{H}$, then $T_v = D_u \setminus D_v$ and $T_w = D_u \setminus D_w$ are both elements of $\widetilde{\mathcal{F}}'$, so they must be edge disjoint. Thus, the orientation D_z obtained from reversing the edges of T_w in D_v or equivalently T_v in D_w is in $O(G, D_0)$. This gives (U2). The same reasoning gives (L2). It remains to show that $\mathcal{H}$ is connected.

Given a 0-homologous oriented subgraph T of G, such that $T = \sum_{F \in \mathcal{F}'} \lambda_F \phi(F)$, we define $s(T) = \sum_{F \in \mathcal{F}'} |\lambda_F|$.

Let D, D' be two orientations in $O(G, D_0)$, and $T = D \setminus D'$. We prove by induction on $s(T)$ that D, D' are connected in $\mathcal{H}$. This is clear if $s(T) = 0$ as then $D = D'$. So we now assume that $s(T) \neq 0$ and so that D, D' are distinct. Lemma 4.9 implies that there exists edge-disjoint oriented subgraphs $T_1, \ldots, T_k$ of D such that $\phi(T) = \sum_{1 \leq i \leq k} \phi(T_i)$, and, for $1 \leq i \leq k$, there exists $\widetilde{X_i} \subseteq \widetilde{\mathcal{F}}'$ and $\epsilon_i \in \{-1, 1\}$ such that $\phi(T_i) = \epsilon_i \sum_{\widetilde{F} \in \widetilde{X_i}} \phi(\widetilde{F})$. Lemma 4.10 applied to T_1 implies that there exists $\widetilde{F_1} \in \widetilde{X_1}$ such that $\epsilon_1 \phi(\widetilde{F_1})$ corresponds to an oriented subgraph of D. Let T' be the oriented subgraph such that $\phi(T) = \epsilon_1 \phi(\widetilde{F_1}) + \phi(T')$. Thus:

$$
\begin{aligned}
\phi(T') &= \phi(T) - \epsilon_1 \phi(\widetilde{F_1}) \\
&= \sum_{1 \leq i \leq k} \phi(T_i) - \epsilon_1 \phi(\widetilde{F_1}) \\
&= \sum_{\widetilde{F} \in (\widetilde{X_1} \setminus \{\widetilde{F_1}\})} \epsilon_1 \phi(\widetilde{F}) + \sum_{2 \leq i \leq k} \sum_{\widetilde{F} \in \widetilde{X_i}} \epsilon_i \phi(\widetilde{F}) \\
&= \sum_{\widetilde{F} \in (\widetilde{X_1} \setminus \{\widetilde{F_1}\})} \sum_{F \in X_{\widetilde{F}}} \epsilon_1 \phi(F) + \sum_{2 \leq i \leq k} \sum_{\widetilde{F} \in \widetilde{X_i}} \sum_{F \in X_{\widetilde{F}}} \epsilon_i \phi(F)
\end{aligned}
$$

So T' is 0-homologous. Let D'' be such that $\epsilon_1 \widetilde{F_1} = D \setminus D''$. So we have $D'' \in O(G, D_0)$ and there is an edge between D and D'' in $\mathcal{H}$. Moreover $T' = D'' \setminus D'$ and $s(T') = $

$s(T) - |X_{\widetilde{F_1}}| < s(T)$. So the induction hypothesis on D'', D' implies that they are connected in $\mathcal{H}$. So D, D' are also connected in $\mathcal{H}$. □

Note that Proposition 4.12 gives a proof of Theorem 4.7 independent from Propp [24]. We continue to further investigate the set $O(G, D_0)$.

Proposition 4.13 *For every element $\widetilde{F} \in \widetilde{\mathcal{F}}$, there exists D in $O(G, D_0)$ such that $\widetilde{F}$ is an oriented subgraph of D.*

Proof. Let $\widetilde{F} \in \widetilde{\mathcal{F}}$. Let D be an element of $O(G, D_0)$ that maximizes the number of edges of $\widetilde{F}$ that have the same orientation in $\widetilde{F}$ and D, i.e. D maximizes the number of edges oriented counterclockwise on the boundary of the face of $\widetilde{G}$ corresponding to $\widetilde{F}$. Towards a contradiction, suppose that there is an edge e of $\widetilde{F}$ that does not have the same orientation in $\widetilde{F}$ and D. The edge e is in $\widetilde{G}$ so it is non-rigid. Let $D' \in O(G, D_0)$ such that e is oriented differently in D and D'. Let $T = D \setminus D'$. By Lemma 4.9, there exist edge-disjoint oriented subgraphs $T_1, \ldots, T_k$ of D such that $\phi(T) = \sum_{1 \le i \le k} \phi(T_i)$, and, for $1 \le i \le k$, there exists $\widetilde{X}_i \subseteq \widetilde{\mathcal{F}}'$ and $\epsilon_i \in \{-1, 1\}$ such that $\phi(T_i) = \epsilon_i \sum_{\widetilde{F}' \in \widetilde{X}_i} \phi(\widetilde{F}')$. W.l.o.g., we can assume that e is an edge of T_1. Let D'' be the element of $O(G, D_0)$ such that $T_1 = D \setminus D''$. The oriented subgraph T_1 intersects $\widetilde{F}$ only on edges of D oriented clockwise on the border of $\widetilde{F}$. So D'' contains strictly more edges oriented counterclockwise on the border of the face $\widetilde{F}$ than D, a contradiction. So all the edges of $\widetilde{F}$ have the same orientation in D. So $\widetilde{F}$ is a 0-homologous oriented subgraph of D. □

By Proposition 4.13, for every element $\widetilde{F} \in \widetilde{\mathcal{F}}'$ there exists D in $O(G, D_0)$ such that $\widetilde{F}$ is an oriented subgraph of D. Thus there exists D' such that $\widetilde{F} = D \setminus D'$ and D, D' are linked in $\mathcal{H}$. Thus, $\widetilde{\mathcal{F}}'$ is a minimal set that generates the lattice.

A distributive lattice has a unique maximal (resp. minimal) element. Let $D_{\max}$ (resp. $D_{\min}$) be the maximal (resp. minimal) element of $(O(G, D_0), \le_{f_0})$.

Proposition 4.14 *$\widetilde{F}_0$ (resp. $-\widetilde{F}_0$) is an oriented subgraph of $D_{\max}$ (resp. $D_{\min}$).*

Proof. By Proposition 4.13, there exists D in $O(G, D_0)$ such that $\widetilde{F}_0$ is an oriented subgraph of D. Let $T = D \setminus D_{\max}$. Since $D \le_{f_0} D_{\max}$, the characteristic flow of T can be written as a combination with positive coefficients of characteristic flows of $\widetilde{\mathcal{F}}'$, i.e. $\phi(T) = \sum_{\widetilde{F} \in \widetilde{\mathcal{F}}'} \lambda_F \phi(\widetilde{F})$ with $\lambda \in \mathbb{N}^{|\widetilde{\mathcal{F}}'|}$. So T is disjoint from $\widetilde{F}_0$. Thus $\widetilde{F}_0$ is an oriented subgraph of $D_{\max}$. The proof is analogous for $D_{\min}$. □

Proposition 4.15 *$D_{\max}$ (resp. $D_{\min}$) contains no counterclockwise (resp. clockwise) non-empty 0-homologous oriented subgraph.*

Proof. Towards a contradiction, suppose that $D_{\max}$ contains a counterclockwise non-empty 0-homologous oriented subgraph T. Then there exists $D \in O(G, D_0)$ distinct from $D_{\max}$ such that $T = D_{\max} \setminus D$. We have $D_{\max} \leq_{f_0} D$ by definition of $\leq_{f_0}$, a contradiction to the maximality of $D_{\max}$. □

In the definition of counterclockwise (resp. clockwise) non-empty 0-homologous oriented subgraph, used in Proposition 4.15, the sum is taken over elements of $\mathcal{F}'$ and thus does not use F_0. In particular, $D_{\max}$ (resp. $D_{\min}$) may contain regions whose boundary is oriented counterclockwise (resp. clockwise) according to the region but then such a region contains F_0.

We conclude this section by applying Theorem 4.7 to Schnyder orientations:

Theorem 4.16 *Let G be a map on an orientable surface given with a particular Schnyder orientation D_0 of $\hat{G}$ and a particular face f_0 of $\hat{G}$. Let $S(\hat{G}, D_0)$ be the set of all the Schnyder orientations of $\hat{G}$ that have the same outdegrees and same type as D_0. We have that $(S(\hat{G}, D_0), \leq_{f_0})$ is a distributive lattice.*

Proof. By the third item of Theorem 4.6, we have $S(\hat{G}, D_0) = O(\hat{G}, D_0)$. Then the conclusion holds by Theorem 4.7. □

Theorem 4.16 is illustrated in Section 5.3 on an example. Note that the minimal element of the lattice and its properties (Proposition 4.12 to 4.15) are used in [7] to obtain a new bijection concerning toroidal triangulations.

5 Toroidal triangulations

5.1 New proof of the existence of Schnyder woods

In this section we look specifically at the case of toroidal triangulations. We study the structure of 3-orientations of toroidal triangulations and show how one can use it to prove the existence of Schnyder woods in toroidal triangulations. This corresponds to the case $g = 1$ of Conjecture 2.14. Given a toroidal triangulation G, a *3-orientation* of G is an orientation of the edges of G such that every vertex has outdegree exactly three. By Theorem 2.12, a simple toroidal triangulation admits a 3-orientation. This can be shown to be true also for non-simple triangulations, for example using edge-contraction.

Consider a toroidal triangulation G and a 3-orientation of G. Let G^∞ be the universal cover of G.

Lemma 5.1 *A cycle C of G^∞ of length k has exactly $k - 3$ edges leaving C and directed towards the interior of C.*

Proof. Let x be the number of edges leaving C and directed towards the interior of C. Consider the cycle C and its interior as a planar graph C^o. Euler's formula gives

$n - m + f = 2$ where n, m, f are respectively the number of vertices, edges and faces of C^o. Every inner vertex has exactly outdegree three, so $m = 3(n - k) + k + x$. Every inner face is a triangle so $2m = 3(f - 1) + k$. The last two equalities can be used to replace f and m in Euler's formula, and obtain $x = k - 3$. $\qquad \square$

For an edge e of G, we define the *middle walk from e* as the sequence of edges $(e_i)_{i \geq 0}$ obtained by the following method. Let $e_0 = e$. If the edge e_i is entering a vertex v, then the edge e_{i+1} is chosen in the three edges leaving v as the edge in the "middle" coming from e_i (i.e. v should have exactly one edge leaving on the left of the path consisting of the two edges e_i, e_{i+1} and thus exactly one edge leaving on the right).

A directed cycle M of G is said to be a *middle cycle* if every vertex v of M has exactly one edge leaving v on the left of M (and thus exactly one edge leaving v on the right of M). Note that if M is a middle cycle, and e is an edge of M, then the middle walk from e consists of the sequence of edges of M repeated periodically. Note that a middle cycle is not contractible, otherwise in G^∞ it forms a contradiction to Lemma 5.1. Similar arguments lead to:

Lemma 5.2 *Two middle cycles that are weakly homologous are either vertex-disjoint or equal.*

We have the following useful lemma concerning middle walks and middle cycles:

Lemma 5.3 *A middle walk always ends on a middle cycle.*

Proof. Start from any edge e_0 of G and consider the middle walk $W = (e_i)_{i \geq 0}$ from e_0. The graph G has a finite number of edges, so some edges will be used several times in W. Consider a minimal subsequence $e_k, \ldots, e_\ell$ such that no edge appears twice and $e_k = e_{\ell+1}$. Thus W ends periodically on the sequence of edges $e_k, \ldots, e_\ell$. We prove that $e_k, \ldots, e_\ell$ is a middle cycle.

Assume that $k = 0$ for simplicity. Thus $e_0, \ldots, e_\ell$ is an Eulerian subgraph E. If E is a cycle then it is a middle cycle and we are done. So we can consider that it visits some vertices several times. Let e_i, e_j, with $0 \leq i < j \leq \ell$, such that e_i, e_j are both leaving the same vertex v. By definition of ℓ, we have $e_i \neq e_j$. Let A and B be the two closed walks $e_i, \ldots, e_{j-1}$ and $e_j, \ldots, e_{i-1}$, respectively, where indices are modulo $\ell + 1$.

Consider a copy v_0 of v in the universal cover G^∞. Define the walk P obtained by starting at v_0 following the edges of G^∞ corresponding to the edges of A, and then to the edges of B. Similarly, define the walk Q obtained by starting at v_0 following the edges of B, and then the edges of A. The two walks P and Q both start at v_0 and both end at the same vertex v_1 that is a copy of v. Note that v_1 and v_0 may coincide. All the vertices that are visited on the interior of P and Q have exactly one edge leaving on the left and exactly one edge leaving on the right. The two walks P and Q may intersect before they end at v_1 thus we define P' and Q' has the subwalks of P and Q starting at v_0, ending on the same vertex u (possibly distinct from v_1 or not) and such that P' and

Q' are not intersecting on their interior vertices. Then the union of P' and Q' forms a cycle C of G^∞. All the vertices of C except possibly v_0 and u, have exactly one edge leaving C and directed towards the interior of C, a contradiction to Lemma 5.1. $\square$

A consequence of Lemma 5.3 is that any 3-orientation of a toroidal triangulation has a middle cycle. The 3-orientation of the toroidal triangulation on the left of Figure 5 is an example where there is a unique middle cycle (the diagonal). We show in Lemma 5.5 that for any toroidal triangulation there exists a 3-orientation with several middle cycles.

Note that a middle cycle C satisfies $\gamma(C) = 0$ (when C is considered in any direction). So, by Lemma 5.3, there is always a cycle with value γ equal to 0 in a 3-orientation of a toroidal triangulation.

The orientation of the toroidal triangulation on the left of Figure 5 is an example of a 3-orientation of a toroidal triangulation where some cycles have value γ not equal to 0. The value of γ for the three loops is $2, 0$ and -2.

Two non-contractible not weakly homologous cycles generate the homology of the torus with respect to $\mathbb{Q}$. That is if B_1, B_2 are non contractible cycles that are not weakly homologous, then for any cycle C there exists $k, k_1, k_2 \in \mathbb{Z}$, $k \neq 0$, such that kC is homologous to $k_1 B_1 + k B_2$.

Lemma 5.4 *In a 3-orientation, consider B_1, B_2, C are non contractible cycles, such that B_1, B_2 are not weakly homologous. Let $k, k_1, k_2 \in \mathbb{Z}$, $k \neq 0$ such that kC is homologous to $k_1 B_1 + k_2 B_2$. Then $k\gamma(C) = k_1\,\gamma(B_1) + k_2\,\gamma(B_2)$.*

Proof. Let v be a vertex in the intersection of B_1 and B_2. Consider a drawing of G^∞ obtained by replicating a flat representation of G to tile the plane. Let v_0 be a copy of v. Consider the path B starting at v_0 and following k_1 times the edges corresponding to B_1 and then k_2 times the edges corresponding to B_2 (we are going backwards if k_i is negative). This path ends at a copy v_1 of v. Since C is non-contractible we have k_1 or k_2 not equal to 0 and thus v_1 is distinct from v_0. Let B^∞ be the infinite path obtained by replicating B (forwards and backwards) from v_0. Since kC is homologous to $k_1 B_1 + k_2 B_2$ we can find an infinite path C^∞, that corresponds to copies of C replicated, that does not intersect B^∞ and situated on the right side of B. Now we can find a copy B'^∞ of B^∞, such that C^∞ lies between B^∞ and B'^∞ without intersecting them. Choose a copy v_0' of v on B'^∞. Let B' be the copy of B starting at v_0' and ending at a vertex v_1'. Let R be the region bounded by B, B' and the segments $[v_0, v_0'], [v_1, v_1']$.

Consider the toroidal triangulation H whose representation is R (obtained by identifying B, B' and $[v_0, v_0'], [v_1, v_1']$). Note that H is just made of several copies of G. Let C' be the subpath of C^∞ intersecting the region R corresponding to exactly one copy of kC. Let R_1 be the subregion of R bounded by B and C' and R_2 the subregion of R bounded by B' and C'. By some counting arguments (Euler's formula + triangulation + 3-orientation) in the region R_1 and R_2, we obtain that $\gamma(C') = \gamma(B)$ and thus $k\gamma(C) = k_1\gamma(B_1) + k_2\gamma(B_2)$. $\square$

By Lemma 5.3, a middle walk W always ends on a middle cycle. Let us denote by M_W this middle cycle and P_W the part of W before M_W. Note that P_W may be empty. We say that a middle walk is leaving a cycle C if its starting edge is incident to C and leaving C.

Let us now prove the main lemma of this section.

Lemma 5.5 *G admits a 3-orientation with two middle cycles that are not weakly homologous.*

Proof. Towards a contradiction, suppose that there is no 3-orientation of G with two middle cycles that are not weakly homologous. We first prove the following claim:

Claim 5.6 *There exists a 3-orientation of G with a middle cycle M, a middle walk W leaving M and $M_W = M$.*

Proof. Towards a contradiction, suppose that there is no 3-orientation of G with a middle cycle M, a middle walk W leaving M and $M_W = M$. We first prove the following:

(1) Any 3-orientation of G, middle cycle M and middle walk W leaving M are such that M does not intersect the interior of W.

Towards a contradiction, suppose that M intersects the interior of W. By assumption, cycles M_W and M are weakly homologous and $M_W \neq M$. Thus by Lemma 5.2, they are vertex-disjoint. So M intersects the interior of P_W. Assume by symmetry that P_W is leaving M on its left side. If P_W is entering M from its left side, in G^∞, the edges of P_W plus M form a cycle contradicting Lemma 5.1. So P_W is entering M from its right side. Hence M_W intersects the interior of P_W on a vertex v. Let e be the edge of P_W leaving v. Then the middle cycle M_W and the middle walk W' started on e satisfies $M_{W'} = M_W$, contradicting the hypothesis. So M does not intersect the interior of W. This proves (1).

Consider a 3-orientation, a middle cycle M and a middle walk W leaving M such that the length of P_W is maximized. By assumption M_W is weakly homologous to M. Assume by symmetry that P_W is leaving M on its left side. By assumption $M_W \neq M$. (1) implies that M does not intersect the interior of W. Let v (resp. e_0) be the starting vertex (resp. edge) of W. Consider now the 3-orientation obtained by reversing M_W. Consider the middle walk W' started at e_0. Walk W' follows P_W, then arrives on M_W and crosses it (since M_W has been reversed). (1) implies that M does not intersect the interior of W'. Similarly, (1) applied to M_W and $W' \setminus P_W$ (the walk obtained from W' by removing the first edges corresponding to P_W), implies that M_W does not intersect the interior of $W' \setminus P_W$. Thus, $M_{W'}$ is weakly homologous to M_W and $M_{W'}$ is in the interior of the region between M and M_W on the right of M. Thus $P_{W'}$ strictly contains P_W and is thus longer, a contradiction. $\diamond$

By Claim 5.6, consider a 3-orientation of G with a middle cycle M and a middle walk W leaving M such that $M_W = M$. Note that W is leaving M from one side and

33

entering it in the other side, otherwise W and M contradicts Lemma 5.1. Let e_0 be the starting edge of W. Let v, u be the starting and ending point of P_W, respectively, where $u = v$ may occur. Consider the 3-orientation obtained by reversing M. Let Q be the directed path from u to v along M (Q is empty if $u = v$). Let C be the directed cycle $P_W \cup Q$. We compute the value γ of C. If $u \neq v$, then C is almost everywhere a middle cycle, except at u and v. At u, it has two edges leaving on its right side, and at v it has two edges leaving on its left side. So we have $\gamma(C) = 0$. If $u = v$, then C is a middle cycle and $\gamma(C) = 0$. Thus, in any case $\gamma(C) = 0$. Note that furthermore $\gamma(M) = 0$ holds. The two cycles M, C are non contractible and not weakly homologous so any non-contractible cycle of G has γ equal to zero by Lemma 5.4.

Consider the middle walk W' from e_0. By assumption $M_{W'}$ is weakly homologous to M. The beginning $P_{W'}$ is the same as for P_W. As we have reversed the edges of M, when arriving on u, path $P_{W'}$ crosses M and continues until reaching $M_{W'}$. Thus $M_{W'}$ intersects the interior of $P_{W'}$ at a vertex v'. Let u' be the ending point of $P_{W'}$ (note that we may have $u' = v'$). Let P' be the non-empty subpath of $P_{W'}$ from v' to u'. Let Q' be the directed path from u' to v' along $M_{W'}$ (Q' is empty if $u' = v'$). Let C' be the non-contractible directed cycle $P' \cup Q'$. We compute $\gamma(C')$. The cycle C' is almost everywhere a middle cycle, except at v'. At v', it has two edges leaving on its left or right side, depending on $M_{W'}$ crossing $P_{W'}$ from its left or right side. Thus, we have $\gamma(C') = \pm 2$, a contradiction. □

By Lemma 5.5, for any toroidal triangulation, there exists a 3-orientation with two middle cycles that are not weakly homologous. By Lemma 5.4, any non-contractible cycle of G has value γ equal to zero. Note that $\gamma(C) = 0$ for any non-contractible cycle C does not necessarily imply the existence of two middle cycle that are not weakly homologous. The 3-orientation of the toroidal triangulation of Figure 15 is an example where $\gamma(C) = 0$ for any non-contractible cycle C but all the middle cycle are weakly homologous. The colors should help the reader to compute all the middle cycles by starting from any edge and following the colors. One can see that all the middle cycles are vertical (up or down) and that the horizontal (non-directed) cycle has value γ equal to 0 so we have γ equal to 0 everywhere. Of course, the colors also show the underlying Schnyder wood.
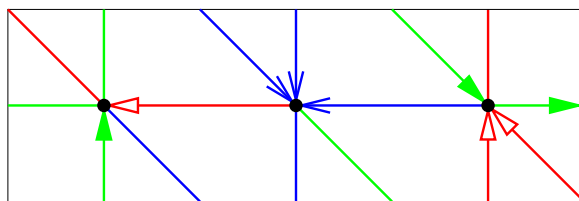

Figure 15: A 3-orientation of a toroidal triangulation with $\gamma(C) = 0$ for any non-contractible cycle C. All the middle cycle are weakly homologous.

By combining Lemma 5.5 and Theorem 3.7, we obtain the following:

Theorem 5.7 *A toroidal triangulation admits a 1-*EDGE*, 1-*VERTEX*, 1-*FACE* angle labeling and thus a Schnyder wood.*

Proof. By Lemma 5.5, there exists a 3-orientation with two middle cycles that are not weakly homologous. By Lemma 5.4, any non-contractible cycle of G has value γ equal to zero. Thus by Theorem 3.7, this implies that the orientation corresponds to an EDGE angle labeling. Then by Lemma 2.1, the labeling is also VERTEX and FACE. As all the edges are oriented in one direction only, it is 1-EDGE. As all the vertices have outdegree three, it is 1-VERTEX. Finally as all the faces are triangles it is 1-FACE (in the corresponding orientation of $\hat{G}$, all the edges incident to dual-vertices are outgoing). By Proposition 2.7, this 1-EDGE, 1-VERTEX, 1-FACE angle labeling corresponds to a Schnyder wood. □

Theorem 5.7 corresponds to the case $g = 1$ of Conjecture 2.14. By [17], we already knew that Schnyder woods exist for toroidal triangulations, but this section provides an alternative proof based on the structure of 3-orientations and the characterization theorem of Section 3.

5.2   The crossing property

A Schnyder wood of a toroidal triangulation is *crossing*, if for each pair i, j of different colors, there exist a monochromatic cycle of color i intersecting a monochromatic cycle of color j. In [17] a strengthening of Theorem 5.7 is proved :

Theorem 5.8 ([17]) *An essentially 3-connected toroidal map admits a crossing Schnyder wood.*

Theorem 5.8 is stronger than Theorem 5.7 for two reasons. First, it considers essentially 3-connected toroidal maps and not only triangulations, thus it proves Conjecture 2.15 for $g = 1$. Second, it shows the existence of crossing Schnyder woods.

However, what we have done in Section 5.1 for triangulation can be generalized to essentially 3-connected toroidal maps. For that purpose one has to work in the primal-dual completion. Proofs get more technical and instead of walks in the primal now walks in the dual of the primal-dual completion have to be considered. This is why we restrict ourselves to triangulations.

Even if we did not prove the existence of crossing Schnyder woods, Lemma 5.5 gives a bit of crossing in the following sense. A 3-orientation obtained by Lemma 5.5 has two middle cycles that are not weakly homologous. Thus in the corresponding Schnyder wood, these two cycles correspond to two monochromatic cycles that intersect. We say that the Schnyder wood obtained by Theorem 5.7 is *half-crossing*, i.e., there exists a pair i, j of different colors, such that there exist a monochromatic cycle of color i intersecting a monochromatic cycle of color j.

A half-crossing Schnyder wood is not necessarily crossing. The 3-orientation of the toroidal triangulation of Figure 16 is an example where two middle cycles are not weakly homologous, so it corresponds to a half-crossing Schnyder wood. However, It is not crossing because the green and the blue cycle do not intersect.
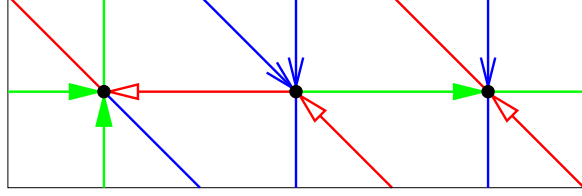

Figure 16: A not crossing but half-crossing Schnyder wood of a toroidal triangulation.

Consider a toroidal triangulation G and a pair $\{B_1, B_2\}$ of cycles that form a basis for the homology. Figure 14 shows how to transform an orientation of G into an orientation of $\hat{G}$. With this transformation a Schnyder wood of G naturally corresponds to a Schnyder orientation of $\hat{G}$. This allows us to not distinguish between a Schnyder wood or the corresponding Schnyder orientation of $\hat{G}$. Recall from Section 4.1, that the type of a Schnyder orientation of $\hat{G}$ in the basis $\{B_1, B_2\}$ is the pair $(\gamma(B_1), \gamma(B_2))$.

Lemma 5.9 *A half-crossing Schnyder wood is of type $(0,0)$ (for the considered basis).*

Proof. Consider a half-crossing Schnyder wood of G and C_1, C_2 two crossing monochromatic cycles. We have $\gamma(C_1) = \gamma(C_2) = 0$. The cycles C_1, C_2 are not contractible and not weakly-homologous. So by Lemma 5.4, any non-contractible cycle C of G satisfies $\gamma(C) = 0$. Thus $\gamma(B_1) = \gamma(B_2) = 0$. □

A consequence of Lemma 5.9 is the following:

Theorem 5.10 *Let G be a toroidal triangulation, given with a particular half-crossing Schnyder wood D_0, then the set $T(G, D_0)$ of all Schnyder woods of G that have the same type as D_0 contains all the half-crossing Schnyder woods of G.*

Recall from Section 4.2, that the set $T(G, D_0)$ carries the structure of a distributive lattice. This lattice contains all the half-crossing Schnyder woods. It shows the existence of a canonical lattice useful for bijection purpose, see [7].

Note that $T(G, D_0)$ may contain Schnyder woods that are not half-crossing. The Schnyder wood of Figure 15 is an example where $\gamma(C) = 0$ for any non-contractible cycle C. So it is of the same type as any half-crossing Schnyder wood but it is not half-crossing.

Note also that in general there exist Schnyder woods not in $T(G, D_0)$. The Schnyder wood of Figure 17 is an example where the horizontal cycle has γ equal to ± 6. Thus it cannot be of the same type as a half-crossing Schnyder wood.
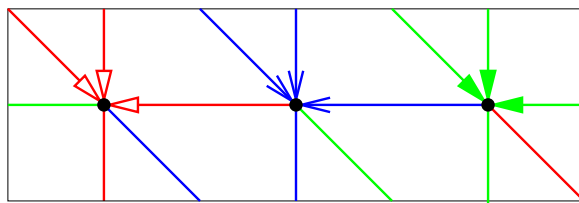
36

Figure 17: A Schnyder wood of a toroidal triangulation where $\gamma(C) \neq 0$ for a non-contractible cycle C.

5.3 A lattice example

Figure 18 illustrates the Hasse diagram of the set $T(G, D_0)$ for the toroidal triangulation G of Figure 16. Bold black edges are the edges of the Hasse diagram $\mathcal{H}$. Each node of the diagram is a Schnyder wood of G. Since we are considering a triangulation $\hat{G}$ is not represented in the figure. Indeed, all the edges of $\hat{G}$ incident to dual-vertices are outgoing in any Schnyder orientation of G, thus these edges are rigid and do not play a role for the structure of the lattice. In every Schnyder wood, a face is dotted if its boundary is directed. In the case of the special face f_0 the dot is black. Otherwise, the dot is magenta if the boundary cycle is oriented counterclockwise and cyan otherwise. An edge in the Hasse diagram from D to D' (with $D \leq D'$) corresponds to a face oriented counterclockwise in D whose edges are reversed to form a face oriented clockwise in D', i.e., a magenta dot is replaced by a cyan dot. The outdegree of a node is its number of magenta dots and its indegree is its number of cyan dots. By Proposition 4.13, all the faces have a dot at least once. The special face is not allowed to be flipped, it is oriented counterclockwise in the maximal Schnyder wood and clockwise in the minimal Schnyder wood by Proposition 4.14. By Proposition 4.15, the maximal (resp. minimal) Schnyder wood contains no other faces oriented counterclockwise (resp. clockwise), indeed in contains only cyan (resp. magenta) dots. The words "no", "half", "full" correspond to Schnyder woods that are not half-crossing, half-crossing (but not crossing), and crossing, respectively. By Theorem 5.10, the figure contains all the half-crossing Schnyder woods of G. The minimal element is the Schnyder wood of Figure 15, and its neighbor is the Schnyder wood of Figure 16.

The graph is very symmetric so the lattice does not depend on the choice of special face. In the example the two crossing Schnyder woods lie in the "middle" of the lattice. These Schnyder woods are of particular interests for graph drawing (see [17]) whereas the minimal Schnyder wood (not crossing in this example) is important for bijective encoding (see [7]).

The underlying toroidal triangulation of Figure 18 has only two Schnyder woods not depicted in Figure 18. One of them two Schnyder wood is shown in Figure 17 and the other one is a 180°rotation of Figure 17. Each of these Schnyder wood is alone in its lattice of homologous orientations. All their edges are rigid. They have no 0-homologous oriented subgraph.
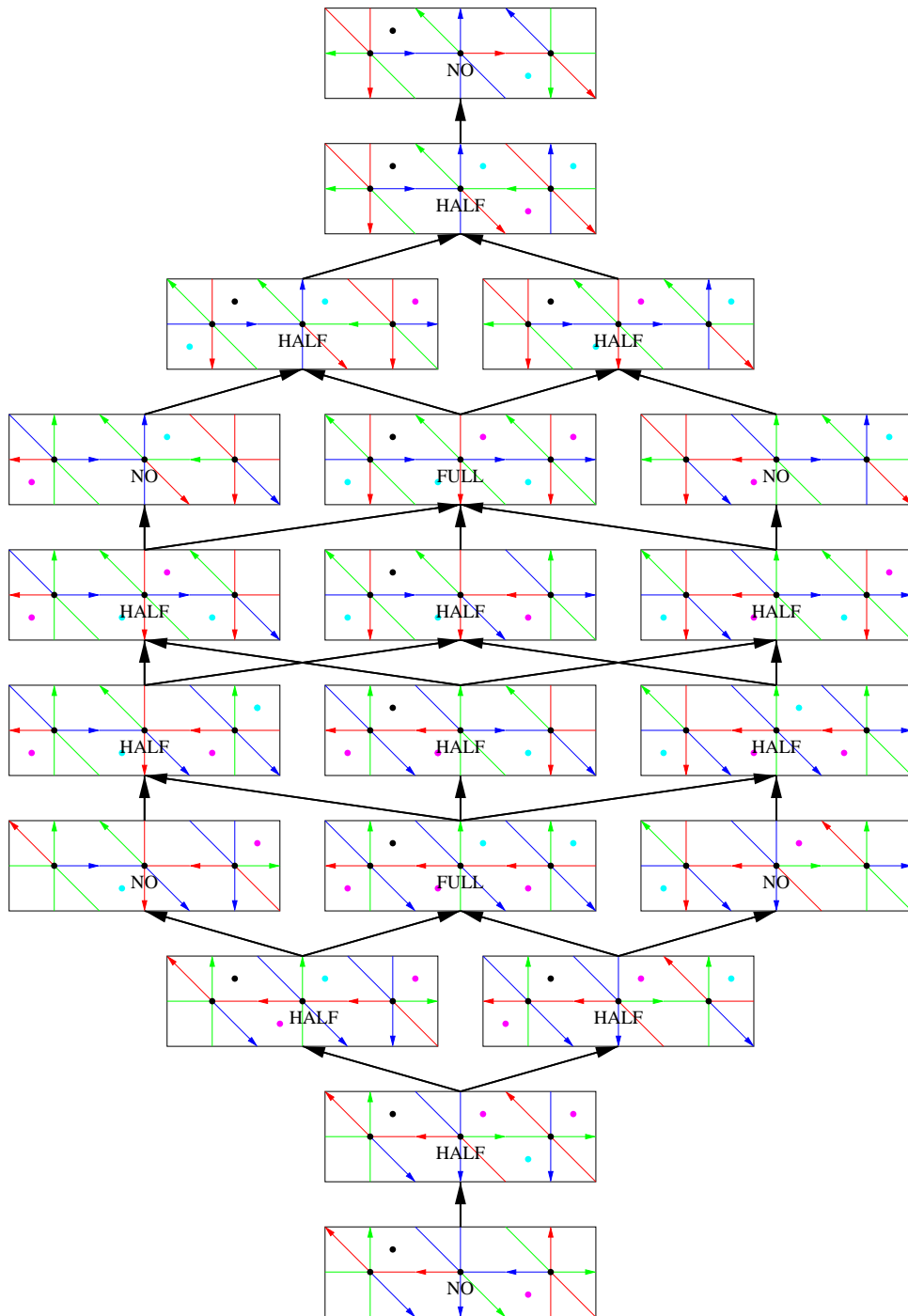
Figure 18: Example of the Hasse diagram of the distributive lattice of homologous orientations of a toroidal triangulation.

Theorem 4.6 says that one can take the Schnyder wood of Figure 17, reverse three or six vertical cycle (such cycles form an Eulerian-partitionable oriented subgraph) to obtain another Schnyder wood. Indeed, reversing any three of these cycles leads to one of the Schnyder wood of Figure 18 (for example reversing the three loops leads to the crossing Schnyder wood of the bottom part). Note that $\binom{3}{6} = 20$ and there are exactly twenty Schnyder woods on Figure 18. Reversing six cycles leads to the same picture pivoted by 180°.

6 Conclusions

In this paper we propose a generalization of Schnyder woods to higher genus via angle labelings. We show that these objects behave nicely with simple characterization theorems and strong structural properties. Unfortunately, we are not able to prove that every essentially 3-connected map admits a generalized Schnyder wood.

As mentioned earlier, planar Schnyder woods have applications in various areas. In the toroidal case, they already lead to some results concerning graph drawing [17] and optimal encoding [7]. It would be interesting to see which other applications can be generalized to higher genus.

Note also that the distributive lattice structure of homologous orientations of a given map (see Theorem 4.7) is a very general result that may be useful to study other objects (transversal structures, $\frac{d}{d-2}$-orientations, etc.) associated to other kinds of maps (4-connected triangulations, d-angulations, etc.).

References

[1] B. Albar, D. Gonçalves, K. Knauer, Orienting triangulations, manuscript, 2014, arXiv:1412.4979.

[2] J. Barát, C. Thomassen, Claw-decompositions and Tutte-orientations, Journal of Graph Theory 52 (2006) 135-146.

[3] J. Barbay, L. Castelli Aleardi, M. He, J. I. Munro, Succinct representation of labeled graphs, Algorithmica 61 (2012) 224-257.

[4] N. Bonichon, A bijection between realizers of maximal plane graphs and pairs of non-crossing Dyck paths, *Discrete Mathematics* 298 (2005) 104-114.

[5] N. Bonichon, C. Gavoille, N. Hanusse, D. Ilcinkas, Connections between Theta-Graphs, Delaunay Triangulations, and Orthogonal Surfaces. WG10 (2010).

[6] L. Castelli Aleardi, E. Fusy, T. Lewiner, Schnyder woods for higher genus triangulated surfaces, with applications to encoding, *Discrete and Computational Geometry* 42 (2009) 489-516.

[7] V. Despré, D. Gonçalves, B. Lévêque, Encoding toroidal triangulations, manuscript, 2015, arXiv:1507.05461.

[8] S. Felsner, Convex Drawings of Planar Graphs and the Order Dimension of 3-Polytopes, *Order* 18 (2001) 19-37.

[9] S. Felsner, Geodesic Embeddings and Planar Graphs, *Order* 20 (2003) 135-150.

[10] S. Felsner, Lattice structures from planar graphs, *Electron. J. Combin.* 11 (2004).

[11] S. Felsner, K. Knauer, ULD-lattices and Δ-bonds, *Comb. Probab. Comput.* 18 5 (2009) 707-724.

[12] S. Felsner, *Geometric Graphs and Arrangements*, Vieweg, 2004.

[13] H. de Fraysseix, P. Ossona de Mendez, P. Rosenstiehl, On Triangle Contact Graphs, *Combinatorics, Probability and Computing* 3 (1994) 233-246.

[14] H. de Fraysseix, P. Ossona de Mendez, On topological aspects of orientations, *Discrete Mathematics* 229 (2001) 57-72.

[15] P. Giblin, *Graphs, surfaces and homology*, Cambridge University Press, Cambridge, third edition, 2010.

[16] D. Gonçalves, B. Lévêque, A. Pinlou, Triangle contact representations and duality, *Discrete and Computational Geometry* 48 (2012) 239-254.

[17] D. Gonçalves, B. Lévêque, Toroidal maps : Schnyder woods, orthogonal surfaces and straight-line representations, *Discrete and Computational Geometry* 51 (2014) 67-131.

[18] G. Kant, Drawing planar graphs using the canonical ordering, *Algorithmica* 16 (1996) 4-32.

[19] W. S. Massey, *Algebraic Topology: An Introduction*, Harcourt, Brace and World, New York, 1967

[20] E. Miller, Planar graphs as minimal resolutions of trivariate monomial ideals, *Documenta Mathematica* 7 (2002) 43-90.

[21] B. Mohar, P. Rosenstiehl, Tessellation and visibility representations of maps on the torus, Discrete Comput. Geom. 19 (1998) 249-263.

[22] P. Ossona de Mendez, Orientations bipolaires, PhD Thesis, Paris, (1994).

[23] D. Poulalhon, G. Schaeffer, Optimal coding and sampling of triangulations, *Algorithmica* 46 (2006) 505-527.

[24] J. Propp, Lattice structure for orientations of graphs, manuscript, 1993, arXiv:math/0209005.

[25] W. Schnyder, Planar graphs and poset dimension, *Order* 5 (1989) 323-343.

[26] W. Schnyder, Embedding planar graphs on the grid, in Proceedings of the First Annual ACM-SIAM Symposium on Discrete Algorithms, *SODA '90* (1990) 138-148.